Copy 6

RM A54I22

NACA RM A54I22

RESEARCH MEMORANDUM

EFFECTS OF RIGID SPOILERS ON THE TWO-DIMENSIONAL FLUTTER

DERIVATIVES OF AIRFOILS OSCILLATING IN PITCH

AT HIGH SUBSONIC SPEEDS

By James C. Monfort and John A. Wyss

Ames Aeronautical Laboratory
Moffett Field, Calif.

CLASSIFICATION CHANGED

UNCLASSIFIED

authority of 4RN-120 Date Aug 13, 1957

N.F.cA Res abs Effective

Amt 10-29-57

NATIONAL ADVISORY COMMITTEE
FOR AERONAUTICS
WASHINGTON
December 17, 1954

NATIONAL ADVISORY COMMITTEE FOR AERONAUTICS

RESEARCH MEMORANDUM

EFFECTS OF RIGID SPOILERS ON THE TWO-DIMENSIONAL FLUTTER

DERIVATIVES OF AIRFOILS OSCILLATING IN PITCH

AT HIGH SUBSONIC SPEEDS

By James C. Monfort and John A. Wyss

SUMMARY

A study was made of the effects of spoilers having fixed heights equal to 2-1/2 and 4 percent of the airfoil chord, on the aerodynamic lift and moment flutter derivatives of two-dimensional airfoils oscillated in pitch about the quarter-chord axis with a mean angle of attack of 2° and an amplitude of $\pm 1^{\circ}$. The reduced frequency varied from 0.045 to 0.45 at 0.5 Mach number and from 0.025 to 0.25 at 0.9 Mach number. The spoilers were affixed at the 70-percent-chord station on the upper surface of airfoils with NACA 65A012, 65A008, 2-008, and 877A008 profiles. The spoilers increased the magnitude of the lift and for some cases the moment derivatives at the higher Mach numbers, particularly at the lower reduced frequencies. The effects on the phase angle of the lift derivative were small, but large changes in the phase angle of the moment derivative occurred. The airfoils with spoilers had negative aerodynamic damping at supercritical speeds, except for the NACA 877A008 airfoil, and the addition of spoilers decreased the Mach number at which a single-degree-of-freedom type of flutter in the torsional mode became a possibility. A comparison of the data for the three models of equal thickness shows, for a given spoiler height, a decrease in the Mach number for torsional instability as the location of the maximum ordinate of the airfoil was moved toward the leading edge. Changing the thickness of the NACA 65A-series airfoil from 8 to 12 percent of the chord significantly reduced the Mach number at which instability occurred for each spoiler height.

INTRODUCTION

The importance of continuing research to determine the dynamic effects of spoilers has been emphasized by the instances of spoiler-induced destructive flutter at sonic speeds reported in reference 1.

The effectiveness of spoilers as lateral-control devices has been the
subject of numerous research investigations. A number of these have
been reported in the papers listed in a bibliography in reference 2.
The authors, however, have knowledge of only two investigations other
than that reported in reference 1 which were concerned with the dynamic
aspects of spoiler-type controls. The first of these investigations was
reported in references 3 and 4, and was concerned with the determination
of flutter speeds and frequencies of a combination of a cusp-type
spoiler, mounted on a three-dimensional wing. The spoiler was free to
oscillate into and out of the air stream. The wing was mounted to pro-
vide for either pitching or rolling motion or flutter. The second
investigation, reported in reference 5, was concerned with the determi-
nation of the oscillatory forces and moments due to the effects of an
oscillating spoiler, acting on a two-dimensional wing fixed at zero
angle of attack. In contrast and complementary to these investigations,
the assumption was made for the purpose of this report that a mechanical
solution to spoiler oscillation was possible in order to simplify and
limit the aerodynamic problem to the effects of fixed spoilers on the
flutter derivatives of oscillating airfoils. This report is therefore
concerned with a study of the effects of spoilers of fixed deflection
on the aerodynamic lift and moment flutter derivatives of two-dimensional
airfoils oscillated in pitch.

SYMBOLS

a velocity of sound in undisturbed air, ft/sec

b wing semichord, ft

c_l dynamic section lift coefficient

c_m dynamic section moment coefficient about quarter point of
                    chord

f frequency of oscillation, cps

i $\sqrt{-1}$

k reduced frequency, $\dfrac{\omega b}{V}$

M Mach number, $\dfrac{V}{a}$

M_α oscillatory aerodynamic section moment on wing about axis
                    of rotation, positive with leading edge up

P_α oscillatory aerodynamic section lift on wing, positive upwards

q   free-stream dynamic pressure, lb/sq ft

V   free-stream velocity, ft/sec

α oscillatory angular displacement (pitch) about axis of
           rotation, positive with leading edge up, radians

α_m mean angle of attack about which oscillation takes place, deg

θ phase angle between oscillatory moment and position α,
           positive for moment leading α, deg

φ phase angle between oscillatory lift and position α,
           positive for lift leading α, deg

ω circular frequency, $2\pi f$, radians/sec

$\left|\dfrac{dc_l}{d\alpha}\right|$ magnitude of dynamic lift-curve slope, $\left|\dfrac{P_\alpha e^{-i\varphi}}{2bq\alpha}\right|$, per radian

$\left|\dfrac{dc_m}{d\alpha}\right|$ magnitude of dynamic moment-curve slope, $\left|\dfrac{M_\alpha e^{-i\theta}}{4b^2 q\alpha}\right|$, per radian

APPARATUS AND METHOD

Tunnel and Model Drive System

A downstream view of the two-dimensional channel in the Ames
16-foot high-speed wind tunnel in which the models were oscillated
and a diagrammatic sketch of the model drive system are shown in
figure 1. The channel was 20 feet long and 16 feet high. The drive
rods, cables, and sector arm attached to the model were contained
within one of the walls.

Models and Instrumentation

Profiles of the NACA 65A012, 2-008, 65A008, and [1]877A008 airfoils
are illustrated in figure 2. A tabulation is also included which
indicates the 15 chord stations at which electrical pressure cells

---

[1]An NACA 847A110 airfoil was modified to a symmetrical section by
using the lower surface coordinates for both upper and lower surfaces
and then reducing the thickness ratio to 8 percent.

were mounted flush with the upper and lower surfaces along the midspan
of each model. A pressure orifice adjacent to each pressure cell was
used to provide an internal reference pressure for each cell through
about 50 feet of 1/16-inch tubing. The pressure orifices were also
used in conjunction with a multiple-tube mercury manometer to determine
steady-state chordwise distributions of pressure. Each model had a
chord of 24 inches and a span of 18-1/4 inches, with the gaps at the
tunnel walls sealed with felt pads or brass strips which moved with the
model.

The same models and associated mechanical and electronic equipment
were used in investigations reported in references 6 and 7, where more
detailed descriptions may be found. Reference 7 contains the results
for the same group of models without spoilers, which will be referred
to herein as results for spoilers of zero height. The two spoilers used
were mounted with the spoiler leading edge at the 70-percent-chord
station. They were made from right-angle aluminum extrusions with one
side machined down to either 2-1/2 or 4 percent of the wing chord. A
4-percent spoiler mounted on the NACA 65A012 model is illustrated in
figure 3.

Method

Data were obtained at from 4 to 40 cps for an amplitude of oscilla-
tion of ±1°. The airfoils were oscillated in pitch about the quarter-
chord axis with a mean angle of attack of 2° and at Mach numbers from
0.5 to 0.9. The reduced frequency varied from 0.045 to 0.45 at 0.5
Mach number, and from 0.025 to 0.25 at 0.9 Mach number. The Reynolds
number varied from 5 million to 8 million. The principal data consisted
of oscillograms recorded on 14-channel oscillographs. Sample oscillograms
for one of the airfoils are shown in figure 4. Traces were recorded
representing the differences in pressure between the upper and lower
surface at each chord station, the lift on the airfoil from a summation
of the electrical output of all cells, and the model angle of attack by
means of an NACA slide-wire transducer. The lift derivatives and phase
angles were evaluated from the fundamental components of 12-point har-
monic analyses of each of three consecutive cycles of the sum traces.
The pitching moments were evaluated by 12-point harmonic analyses of
the individual traces for one cycle.

Because of the effects of wind-tunnel resonance, data taken within
10 percent of the tunnel resonant frequencies have been omitted. (See
refs. 8, 9, and 10.) Although the use of such a procedure does not
mean tunnel-wall effects have been completely eliminated over the entire
frequency range, it is felt that any remaining tunnel-wall effects are
but a small factor in the trends of the data (see ref. 7).

RESULTS

Before presenting the results, it is desired to emphasize the fact that the flutter derivatives contained herein are representative of the slope of the lift and moment curves, rather than of the absolute values of lift and moment. This is illustrated in figure 5, which shows the lift characteristics at zero and low frequencies for the NACA 65A008 airfoil with and without spoilers at 0.59 Mach number. In this figure, the symboled points represent data derived from steady-state pressure distributions measured by means of the pressure orifices and multiple-tube mercury manometer. The dashed lines represent the variation in lift for a frequency of oscillation of about 2 cps. It is obvious from this figure that even though the slopes of all the curves are nearly the same, spoiler deflection resulted in large reductions in the absolute magnitude of the lift forces acting on the wing. Such a reduction occurred on all models over the entire speed range of the investigation.

The measured lift and moment flutter derivatives and their phase angles for fixed spoiler heights of 2-1/2 and 4 percent of the wing chord are presented in tables I, II, III, and IV, for the NACA 2-008, 65A008, 877A008, and 65A012 airfoils, respectively. As previously indicated, corresponding values are tabulated in reference 7 for the airfoils without spoilers.

In figures 6 and 7 are presented the magnitudes and phase angles of the lift and moment derivatives, respectively, for the NACA 65A008 airfoil for two Mach numbers. The derivatives are plotted as functions of reduced frequency to show typical effects of this parameter.

Figures 8, 9, 10, and 11 contain cross plots of the lift derivative and phase angle for fixed spoiler deflections as a function of Mach number for three representative reduced frequencies for the NACA 2-008, 65A008, 877A008, and 65A012 airfoils, respectively.

Figures 12, 13, 14, and 15 contain cross plots of the moment derivative and phase angle presented in the same order as the lift derivatives. This order of presentation was chosen to correspond to the rearward change in the location of maximum thickness for the NACA 2-008, 65A008, and 877A008 airfoils which have maximum ordinates at about 16, 42, and 63 percent of the chord, respectively. Since the NACA 65A008 airfoil is intermediate, it is considered the reference airfoil. The investigation included only two models of different thickness-to-chord ratios, the NACA 65A012 and 65A008 airfoils. The derivatives for the NACA 65A012 airfoil provide some indication of the effects of increasing the thickness of the reference airfoil.

Figures 16 and 17 contain aerodynamic torsional instability boundaries for various spoiler deflections for the three models which

differed in thickness distribution and for the two models which differed in thickness, respectively.

DISCUSSION

Typical Effects of Spoiler Deflection

In figures 6 and 7, the lift and moment flutter derivatives and phase angles are presented as functions of reduced frequency for the reference airfoil, the NACA 65A008. Included in each figure are results for supercritical Mach numbers of 0.68 and 0.84. The critical Mach number for the plain airfoil at an angle of attack of 2° was 0.59, which was calculated from the pressure distributions measured by means of the pressure orifices and multiple-tube mercury manometer.

Included in figures 6 and 7 and in subsequent figures are curves derived from thin-airfoil theory. Theoretical values at Mach numbers of 0.5, 0.6, and 0.7 were obtained from the work of Dietze (refs. 11 and 12), at Mach number of 0.8 from Minhinnick (ref. 13), and at Mach number of 1.0 from Nelson and Berman (ref. 14).

In figure 6 it is perhaps not surprising, in view of the data already presented in figure 5, to see the relatively small effects at 0.68 Mach number of spoilers of fixed heights on the lift derivative and phase angle. At 0.84 Mach number, the largest effects appear to occur at the lower and higher extremes of reduced frequency, although the trends with reduced frequency are similar.

In figure 7 the large variation from theory of the moment derivative phase angle at 0.68 Mach number can be attributed to a center-of-pressure location nearer the leading edge than theory predicts. (See ref. 15.) An increase in Mach number to 0.84 resulted in a greater effect of spoiler deflection on the moment derivative and phase angle than was the case for the lift derivative and phase angle in figure 6. The large shift in the phase angle of the moment derivative is of particular importance in that at reduced frequencies of 0.016 and 0.053, the phase angle shifted from a lagging to a leading phase angle; that is, the phase angle shifted so that $0^\circ < \theta < 180^\circ$. For these instances, the sign of the moment damping component became positive, which means that the aerodynamic damping forces acting on the wing were negative with the possibility of a single-degree-of-freedom type of flutter. It thus appears that the spoiler resulted in a shift from a stable to an unstable condition.

Effects of Mach Number

Figures 6 and 7 indicate that reduced frequency and Mach number each have important effects on the flutter derivatives. Figures 7 through 14 have been prepared to show the salient effects of these parameters. The lift and moment flutter derivatives are presented as functions of Mach number for three reduced frequencies.

Lift derivative and phase angle.- Examination of figures 8 through 11 indicates that the spoilers had a greater effect on the magnitude of the lift derivative than on the phase angle. Although there were exceptions, the effect at the higher Mach numbers was to increase the magnitude of the lift derivative, particularly at the lower values of reduced frequency. A comparison of figure 9 for the NACA 65A008 airfoil with figure 11 for the NACA 65A012 airfoil indicates that the increase in the magnitude of the lift derivative with spoiler deflection was larger for the thicker airfoil. It is interesting to note that at 0.6 Mach number, reasonable agreement was obtained for all spoiler heights with the theory for a wing without spoiler.

In reference 7 it was proposed that the Mach number for lift divergence could be used as an approximate criterion for the Mach number at which large variations in the magnitude of the lift flutter derivative occurred as Mach number was increased. The approximate Mach numbers for lift divergence for the plain airfoils were 0.72, 0.77, 0.76, and 0.68 for the NACA 2-008, 65A008, 877A008, and 65A012 profiles, respectively. Although the Mach number for lift divergence for an airfoil with a spoiler would not be the same, it would appear from figures 8 to 11 that this criterion is still useful, even with a deflected spoiler.

The effect of spoiler height on the phase angle of the lift derivative was small and a definite trend is difficult to detect. It would appear that with or without the spoilers, at the higher Mach numbers an increasing lag of the phase angle of the lift derivative occurred relative to the theoretical values. The change in phase angle was sufficiently small that the theory for a wing without a spoiler is considered to provide a reasonable prediction for the lift-derivative phase angles for the spoiler heights and location investigated.

Moment derivative and phase angle.- It is obvious from examination of figures 12 through 15 that the spoilers had significant effects on the phase angle as well as on the magnitude of the moment derivative. With regard to the magnitude of the moment derivative, it would appear that, again, even though there were exceptions, the spoilers increased the magnitude, particularly at the lower values of reduced frequency, at the higher Mach numbers.

It may be of interest to note that the phase shift in figure 12 could be presented in such a manner as to show an increasing lead of the moment derivative in going from the stable to the unstable condition, rather than an increasing lag. However, it is felt that the Mach number increments at which data were taken were not sufficiently small to clearly define for all cases whether the moment derivative approached the unstable condition by either an increasing lag or increasing lead.

The general effect of the spoilers on the phase angle, with an exception for the NACA 877A008 airfoil, was to decrease the Mach number at which occurred the large shift of approximately 180° from a lagging to a leading phase angle, with a resultant change from a stable to an unstable condition. In figure 12 another exception appears in that a reversal occurred such that instability occurred for the 2-1/2-percent spoiler at Mach numbers less than those for the 4-percent spoiler. No explanation for this exception can be given.

Aerodynamic Torsional Instability Boundaries for Fixed Spoiler Heights as Affected by Airfoil Profile

In order to show the effects of airfoil profile on the Mach numbers at which instability occurred, the Mach numbers at which the moment-derivative phase angle became less than 180° in figures 12 through 15 are presented in figures 16 and 17 in terms of the flutter-speed parameter, $V/\omega b$, the reciprocal of reduced frequency, k. In this manner, what is termed an aerodynamic torsional instability boundary was established. This boundary defines the Mach number for which any further increase in free-stream velocity results in the possibility of torsional single-degree-of-freedom flutter.

Figure 16 contains the boundaries for the three 8-percent-thick models. It may be noted that without a spoiler only the NACA 2-008 airfoil, with the maximum thickness at an extreme forward position, had a boundary within the limits of the investigation. Spoiler deflection for this model resulted in a reduction in Mach number at which instability occurred. The effect of spoilers on the NACA 65A008 airfoil was to cause torsional instability, which otherwise did not occur. In contrast, the NACA 877A008 airfoil was stable throughout the speed range of the investigation. In order to emphasize the effects of thickness distribution, and for this reason only, boundaries based on extrapolation are also included.

The usefulness of figure 16 is twofold: It indicates the effect of spoilers in reducing the Mach number at which instability occurred, and also indicates that this Mach number decreased as the location of the maximum ordinate of the airfoil was moved toward the leading edge.

The boundaries for the NACA 65A012 and NACA 65A008 airfoils are compared in figure 17. As in figure 16, this figure illustrates the reduction in Mach number of the boundary due to spoiler deflection. It also indicates the reduction in Mach number of the boundaries when the thickness of the reference airfoil was increased.

This figure should not be construed to indicate that a reduction of the reference airfoil thickness would necessarily be beneficial in increasing the Mach number of the boundaries. Results presented in reference 7 for an NACA 65A004 airfoil without a spoiler indicate that this airfoil became abruptly unstable at 0.88 Mach number.

CONCLUSIONS

Within the limitations of speed range, reduced frequency, and spoiler height of the investigation, the following conclusions can be drawn:

1. The spoilers increased the magnitude of the lift and for some cases the moment derivatives at the higher Mach numbers, particularly at the lower reduced frequencies. The effects on the phase angle of the lift derivative were small, but large changes in the phase angle of the moment derivative occurred.

2. The airfoils with spoilers had negative aerodynamic damping at supercritical speeds, except for the NACA 877A008 airfoil, and the addition of spoilers decreased the Mach number at which a single-degree-of-freedom type of flutter became a possibility.

3. A comparison of the data for the three models of equal thickness showed, for a given spoiler height, a decrease in the Mach number for torsional instability as the maximum ordinate of the airfoil was moved toward the leading edge.

4. When thickness of the airfoil was increased from 8 percent to 12 percent of the wing chord, the Mach number for instability for each spoiler height was significantly reduced.

Ames Aeronautical Laboratory
    National Advisory Committee for Aeronautics
        Moffett Field, Calif., Sept. 22, 1954

REFERENCES

1. Strass, H. Kurt, and Marley, Edward T.: Recent Experiences with
    Flutter Failure of Sweptback, Tapered Wings Having Outboard,
    Partial-Span Spoiler Controls. NACA RM L53H26, 1953..

2. Lowry, John G.: Data on Spoiler-Type Ailerons. NACA RM L53I24a,
    1953.

3. Johnson, Carl G.: Spoiler Flutter Tests in the Wind Tunnel.
    Wright Air Dev. Center. (Serial) WCNSY-4595-7-4, Mar. 1952.

4. Schwab, R. H., and Fotieo, G.: An Experimental Investigation of
    the Flutter Characteristics of a Cusp-Type Spoiler. Wright Air
    Dev. Center. TR 5785, Jan. 1953.

5. Clevenson, Sherman A., and Tomassoni, John E.: Experimental
    Investigation of the Oscillating Forces and Moments on a Two-
    Dimensional Wing Equipped with an Oscillating Circular-Arc
    Spoiler. NACA RM L53K18, 1954.

6. Coe, Charles F., and Mellenthin, Jack A.: Buffeting Forces on
    Two-Dimensional Airfoils as Affected by Thickness and Thickness
    Distribution. NACA RM A53K24, 1954.

7. Wyss, John A., and Monfort, James C.: Effects of Airfoil Profile
    on the Two-Dimensional Flutter Derivatives for Wings Oscillating
    in Pitch at High Subsonic Speeds. NACA RM A54C24, 1954.

8. Runyan, Harry L., and Watkins, Charles E.: Considerations on the
    Effect of Wind-Tunnel Walls on Oscillating Air Forces for Two-
    Dimensional Subsonic Compressible Flow. NACA TN 2552, 1951.

9. Runyan, Harry L., Woolston, Donald S., and Rainey, A. Gerald: A
    Theoretical and Experimental Study of Wind-Tunnel-Wall Effects
    on Oscillating Air Forces for Two-Dimensional Subsonic Compressible
    Flow. NACA RM L52I17a, 1953.

10. Woolston, Donald S., and Runyan, Harry L.: Some Considerations on
    the Air Forces on a Wing Oscillating Between Two Walls for
    Subsonic Compressible Flow. IAS Preprint No. 446, 1954.

11. Dietze, F.: The Air Forces of the Harmonically Vibrating Wing in
    Compressible Medium at Subsonic Velocity (Plane Problem). AAF,
    Air Mat. Com., Wright Field, Tech. Intelligence. Trans.
    F-TS-506-RE, Nov. 1946.

12. Dietze, F.: The Air Forces of the Harmonically Vibrating Wing in
    a Compressible Medium at Subsonic Velocity (Plane Problem).
    Part II: Numerical Tables and Curves. AAF Air Mat. Com.,
    Wright Field, Tech. Intelligence. Trans. F-TS-948-RE, Mar. 1947.

13. Minhinnick, I. T.: Subsonic Aerodynamic Flutter Derivatives for
    Wings and Control Surfaces (Compressible and Incompressible
    Flow). British R.A.E. Structures 87, July 1950.

14. Nelson, Herbert C., and Berman, Julian H.: Calculations on the
    Forces and Moments for an Oscillating Wing-Aileron Combination
    in Two-Dimensional Potential Flow at Sonic Speed. NACA Rep.
    1128, 1953. (Supersedes NACA TN 2590.)

15. Wyss, John A., and Herrera, Raymond: Effects of Angle of Attack
    and Airfoil Profile on the Two-Dimensional Flutter Derivatives
    for Airfoils Oscillating in Pitch at High Subsonic Speeds.
    NACA RM A54H12, 1954.

TABLE I.— MEASURED FLUTTER DERIVATIVES FOR THE NACA 2-008 AIRFOIL WITH SPOILERS AT THE 70-PERCENT-CHORD STATION ON THE UPPER SURFACE; $\alpha_m = 2^\circ$

		Spoiler height 2-1/2 percent							Spoiler height 4 percent				
M	k	ω	$\frac{dc_l}{d\alpha}$	φ	$\frac{dc_m}{d\alpha}$	θ	M	k	ω	$\frac{dc_l}{d\alpha}$	φ	$\frac{dc_m}{d\alpha}$	θ
0.590	0.041	28.3	6.438	350.5	- - -	- - -	0.590	0.038	26.0	6.669	351.2	- - -	- - -
	.079	54.2	5.801	348.0	- - -	- - -		.077	52.3	5.966	351.8	- - -	- - -
	.111	75.9	5.929	344.5	- - -	- - -		.111	75.5	5.959	352.8	- - -	- - -
	.154	105.4	5.408	349.1	- - -	- - -		.151	102.7	5.616	351.3	- - -	- - -
	.186	127.7	5.339	347.9	- - -	- - -		.187	126.9	5.297	355.1	- - -	- - -
	.226	154.8	5.195	347.4	- - -	- - -		.229	155.1	5.033	349.9	- - -	- - -
	.340	232.7	5.032	2.8	- - -	- - -		.343	232.7	5.205	2.6	- - -	- - -
	.376	257.5	6.413	6.7	- - -	- - -		.370	251.3	6.169	356.9	- - -	- - -
.680	.068	54.3	7.338	347.0	0.612	319.2	.680	.033	26.5	6.936	356.0	0.534	347.0
	.096	75.9	6.787	348.0	- - -	- - -		.066	52.0	6.865	352.5	.608	329.1
	.130	103.5	6.315	338.0	.592	315.9		.096	76.2	6.358	345.9	- - -	- - -
	.161	128.0	5.706	344.3	- - -	- - -		.130	102.7	6.012	347.3	.534	312.6
	.193	152.9	5.512	337.0	.691	296.2		.161	127.4	5.347	346.3	- - -	- - -
	.291	231.0	5.903	357.4	- - -	- - -		.196	154.8	5.253	340.8	.668	276.4
	.327	259.6	7.448	348.8	.950	272.5		.295	232.7	5.730	359.0	- - -	- - -
								.321	253.3	6.539	350.1	1.008	268.1
.728	.034	29.1	7.999	349.2	.561	345.1							
	.062	53.7	7.228	344.1	.819	322.9	.728	.029	24.5	8.094	351.9	.623	340.3
	.089	76.7	6.638	343.8	- - -	- - -		.062	52.8	7.386	345.6	.706	317.4
	.125	107.6	6.326	340.3	.661	311.1		.088	74.9	7.067	344.9	- - -	- - -
	.149	128.5	5.722	338.9	- - -	- - -		.147	125.2	6.127	339.5	- - -	- - -
	.246	211.6	5.321	353.8	.601	287.4		.240	204.6	5.525	359.3	.773	287.8
	.274	235.3	6.311	353.1	- - -	- - -		.270	230.2	6.224	352.2	- - -	- - -
	.303	260.7	6.435	345.8	.980	263.0		.303	258.6	6.519	349.4	1.087	255.4
.787	.034	31.5	12.711	339.3	.077	134.5	.787	.030	27.5	10.108	357.6	.204	347.0
	.056	52.5	10.645	334.9	.156	65.8		.056	51.5	8.755	344.9	.397	322.3
	.079	73.9	8.946	329.4	- - -	- - -		.083	77.1	7.887	339.0	- - -	- - -
	.114	106.7	7.993	323.3	.446	12.2		.112	103.7	7.206	331.7	.503	285.9
	.136	127.4	6.774	325.1	- - -	- - -		.138	128.5	6.423	325.1	- - -	- - -
	.222	208.0	5.947	342.7	.666	319.0		.228	211.6	6.005	343.2	.813	273.0
	.253	237.1	7.021	340.2	- - -	- - -		.252	233.5	6.593	347.5	- - -	- - -
	.273	255.4	7.546	341.3	1.041	290.5		.282	261.8	8.648	357.8	1.310	256.0
.801	.026	25.3	13.428	340.2	- - -	- - -	.801	.027	26.0	13.626	343.2	1.211	149.6
	.052	49.8	11.347	329.0	- - -	- - -		.060	56.9	11.870	324.7	.787	103.0
	.079	75.6	9.962	319.9	- - -	- - -		.082	77.7	9.945	329.7	- - -	- - -
	.107	102.5	8.592	319.9	- - -	- - -		.109	103.7	7.838	326.2	.372	32.5
	.132	126.4	6.985	312.1	- - -	- - -		.136	129.0	6.305	324.7	- - -	- - -
	.185	177.0	5.998	330.2	- - -	- - -		.194	183.7	6.203	342.0	- - -	- - -
	.217	207.3	5.909	328.7	- - -	- - -		.217	206.0	5.816	335.9	.412	301.0
	.249	238.0	6.824	333.5	- - -	- - -		.249	236.2	7.557	345.6	- - -	- - -
	.275	262.9	8.212	327.2	- - -	- - -		.270	256.5	8.706	336.4	1.150	280.0
.835	.030	30.2	13.928	338.5	1.014	158.6	.835	.025	25.1	16.196	333.2	2.380	156.1
	.054	53.9	12.350	323.5	.948	142.8		.053	52.4	12.022	331.3	1.846	127.5
	.076	76.5	10.372	317.6	- - -	- - -		.076	75.5	10.286	324.2	- - -	- - -
	.107	106.9	7.645	311.4	.520	117.8		.107	105.8	7.701	318.4	1.032	124.3
	.186	185.9	5.964	331.6	- - -	- - -		.181	179.0	4.872	326.3	- - -	- - -
	.209	209.4	6.877	330.8	.086	123.1		.210	208.0	5.414	339.0	.126	91.8
	.234	234.4	7.476	331.1	- - -	- - -		.232	230.2	6.728	334.6	- - -	- - -
	.258	258.6	7.855	325.0	.696	228.1		.262	259.6	7.912	329.5	.358	171.0
.857	.027	27.5	15.798	342.8	- - -	- - -	.857	.027	27.7	14.008	340.7	2.626	142.8
	.051	52.7	12.563	323.8	- - -	- - -		.050	50.6	11.568	325.7	2.127	143.5
	.073	75.3	10.644	317.7	- - -	- - -		.074	76.0	9.739	318.5	- - -	- - -
	.102	105.4	8.696	296.8	- - -	- - -		.100	102.4	6.948	310.1	1.417	115.5
	.150	154.4	5.680	331.0	- - -	- - -		.152	155.1	4.915	324.2	.952	116.7
	.177	183.2	5.918	327.7	- - -	- - -		.177	181.1	5.589	330.2	- - -	- - -
	.202	208.0	7.502	333.5	- - -	- - -		.197	201.4	6.113	337.9	.753	129.3
	.231	238.9	8.015	329.2	- - -	- - -		.230	235.3	6.979	331.4	- - -	- - -
	.249	256.5	7.822	316.5	- - -	- - -		.251	256.5	7.692	325.7	.963	127.6
.884	.026	27.5	11.499	342.8	2.062	150.6	.884	.028	29.4	9.025	357.7	2.669	165.5
	.049	52.5	9.413	332.9	1.706	145.6		.050	52.7	8.663	338.9	2.468	141.9
	.071	75.4	8.178	324.2	- - -	- - -		.071	74.5	7.801	336.0	- - -	- - -
	.095	101.3	5.676	316.4	.819	121.9		.100	105.1	5.401	326.7	1.191	110.4
	.142	151.4	5.192	333.1	.692	114.0		.149	157.5	5.245	346.4	.676	139.0
	.170	181.1	5.327	344.5	- - -	- - -		.167	176.5	5.996	341.6	- - -	- - -
	.196	209.4	6.948	336.9	.772	167.5		.197	207.3	6.653	337.3	.978	130.2
	.218	232.7	6.687	330.8	- - -	- - -		.222	234.4	6.394	334.7	- - -	- - -
	.244	260.7	6.996	333.1	.607	162.2		.247	260.7	7.008	324.0	.987	155.7

TABLE II.– MEASURED FLUTTER DERIVATIVES FOR THE NACA 65A008 AIRFOIL WITH SPOILERS AT THE 70-PERCENT-CHORD STATION ON THE UPPER SURFACE; $\alpha_m = 2°$

| | Spoiler height 2-1/2 percent | | | | | | | Spoiler height 4 percent | | | | | |
M	k	ω	$\left\|\dfrac{dc_l}{d\alpha}\right\|$	φ	$\left\|\dfrac{dc_m}{d\alpha}\right\|$	θ	M	k	ω	$\left\|\dfrac{dc_l}{d\alpha}\right\|$	φ	$\left\|\dfrac{dc_m}{d\alpha}\right\|$	θ
0.590	0.029	19.4	7.217	352.0	---	---	0.590	0.050	33.2	5.816	349.9	---	---
	.076	53.2	6.711	352.2	---	---		.081	54.3	5.920	349.7	---	---
	.121	82.4	5.872	351.2	---	---		.118	78.7	5.607	351.0	---	---
	.156	105.6	5.760	349.2	---	---		.159	106.1	5.337	356.4	---	---
	.196	133.1	5.698	351.4	---	---		.195	130.6	5.222	356.7	---	---
	.233	157.9	5.730	351.5	---	---		.239	159.5	4.932	353.1	---	---
	.271	183.7	5.297	347.4	---	---		.273	182.7	4.834	345.0	---	---
	.345	234.4	5.435	3.3	---	---		.351	234.4	4.822	359.0	---	---
	.386	261.8	7.115	354.3	---	---		.387	258.6	6.286	354.0	---	---
.680	.030	23.2	7.729	355.1	0.4675	349.1	.680	.041	32.2	7.398	350.9	---	---
	.066	52.1	6.907	351.2	.5796	328.5		.070	54.7	6.661	349.8	0.334	318.7
	.103	80.7	6.758	344.0	---	---		.105	81.5	6.087	348.5	---	---
	.135	105.8	6.506	344.3	.513	315.0		.138	107.1	5.925	342.4	.392	307.4
	.170	133.1	6.274	341.9	---	---		.172	133.7	5.857	338.9	---	---
	.202	158.3	5.861	337.1	.602	287.9		.205	159.1	5.137	335.1	.540	265.2
	.300	235.3	6.321	358.3	---	---		.304	236.2	5.653	3.4	---	---
	.325	255.4	6.517	349.9	.934	281.2		.335	260.7	6.121	355.7	.899	289.3
.728	.026	21.9	8.237	357.2	.500	342.2	.728	.038	32.2	7.795	349.8	.350	322.8
	.064	53.2	7.667	348.1	.477	325.7		.066	55.5	7.123	345.3	.390	318.4
	.098	81.4	6.947	343.1	---	---		.099	83.3	6.806	345.3	---	---
	.128	106.5	6.723	343.6	.543	311.6		.127	106.9	6.388	345.6	.419	295.5
	.158	131.4	6.251	337.3	---	---		.157	131.4	5.955	341.0	---	---
	.250	208.7	5.502	355.0	.712	291.5		.252	211.6	5.652	356.0	.589	280.4
	.279	232.7	6.729	350.5	---	---		.279	234.4	6.175	355.1	---	---
	.311	259.6	7.296	352.3	1.093	281.4		.312	261.8	7.094	353.1	.994	244.3
.787	.021	19.7	9.162	353.8	.643	348.8	.787	.038	34.5	8.076	356.2	.307	333.3
	.056	51.8	8.748	346.0	.652	318.5		.058	52.8	8.128	350.6	.330	302.5
	.085	78.9	7.988	340.8	---	---		.087	79.0	7.749	343.8	---	---
	.113	104.4	7.153	339.0	.714	287.6		.113	103.0	6.796	333.7	.413	272.5
	.141	130.4	6.853	329.4	---	---		.147	133.6	5.926	335.4	---	---
	.198	182.6	5.834	350.9	---	---		.206	187.6	5.463	352.6	---	---
	.224	206.6	6.156	351.8	.866	294.3		.230	209.4	5.454	351.5	.599	264.3
	.251	231.8	6.994	351.1	---	---		.259	235.3	6.508	353.6	---	---
	.278	256.5	8.392	351.1	1.473	274.7		.284	258.6	8.488	353.8	1.476	250.3
.801	.022	21.0	10.152	352.3	---	---	.801	.034	31.2	8.902	2.6	.195	333.8
	.056	52.7	9.560	342.0	---	---		.056	52.2	8.725	353.7	---	---
	.085	79.9	8.677	338.6	---	---		.086	80.0	8.288	342.7	---	---
	.111	104.7	8.124	335.0	---	---		.113	105.4	7.926	330.6	.406	276.4
	.168	158.3	6.433	331.1	---	---		.139	129.5	6.094	333.0	---	---
	.191	180.0	6.179	342.7	---	---		.199	184.8	5.717	343.6	---	---
	.218	205.3	6.669	350.8	---	---		.228	212.2	6.005	349.0	.629	260.7
	.247	232.7	7.502	351.6	---	---		.258	239.8	8.500	351.3	---	---
	.273	257.5	9.190	348.8	---	---		.281	261.8	9.258	344.5	.872	227.8
.835	.022	21.8	12.331	353.1	.341	350.7	.835	.016	15.8	10.194	354.8	.931	181.9
	.051	50.3	10.938	334.7	.167	299.3		.053	51.1	9.133	347.0	.424	141.0
	.079	77.8	9.250	328.7	---	---		.080	77.0	8.464	334.9	---	---
	.106	104.4	7.723	324.6	.471	280.9		.104	100.8	7.398	327.3	.256	215.1
	.160	156.7	5.092	347.4	.428	300.0		.160	155.1	5.432	351.4	---	---
	.185	181.6	5.918	341.9	---	---		.181	175.5	5.335	348.8	---	---
	.207	202.7	6.541	353.6	1.037	289.5		.207	200.1	6.790	355.1	.755	267.8
	.234	229.3	7.458	351.1	---	---		.236	228.5	7.896	345.1	---	---
	.259	254.4	8.934	335.1	1.776	296.7		.261	252.3	8.606	349.6	.899	216.5
.857	.022	21.8	15.661	342.9	---	---	.857	.053	52.5	11.298	336.2	1.656	126.4
	.053	53.5	11.770	318.7	---	---		.077	76.8	9.138	317.8	---	---
	.079	79.9	8.867	301.7	---	---		.104	103.0	7.285	315.8	.624	93.6
	.104	104.5	6.969	310.7	---	---		.156	154.8	5.041	342.7	.339	139.1
	.152	153.2	4.954	335.6	---	---		.180	178.5	6.001	347.1	---	---
	.180	182.1	4.912	340.5	---	---		.204	202.7	7.254	346.3	.458	197.8
	.201	203.3	6.645	341.1	---	---		.232	231.0	8.318	332.6	---	---
	.229	231.0	6.868	333.1	---	---		.253	251.3	7.483	324.1	.821	142.5
	.257	259.6	7.596	333.9	---	---	.884	.050	51.3	11.663	329.7	1.907	139.8
.884	.018	18.8	15.404	340.9	3.349	151.7		.076	79.0	8.929	321.4	---	---
	.048	49.7	12.099	320.5	2.863	124.9		.098	101.7	6.077	304.1	1.176	94.7
	.076	78.9	8.345	308.7	---	---		.153	158.3	5.613	335.2	.767	92.3
	.101	104.4	6.110	297.4	1.461	52.7		.172	177.5	6.269	335.7	---	---
	.153	160.1	4.575	325.7	.703	41.1		.197	204.0	6.695	339.3	.896	128.6
	.175	181.1	5.128	330.5	---	---		.228	235.3	6.580	326.0	---	---
	.194	200.7	6.151	331.5	.249	273.9		.245	253.4	6.205	331.6	.241	74.9
	.224	231.8	6.331	330.7	---	---							
	.250	258.5	5.998	324.5	.439	130.7							
.902	.018	18.5	11.238	346.2	2.708	178.4							
	.047	49.3	9.850	320.5	2.456	118.4							
	.073	76.8	7.537	321.3	---	---							
	.121	127.2	4.361	334.5	---	---							
	.144	150.7	4.862	346.2	.532	99.1							
	.170	178.0	6.076	349.9	---	---							
	.199	208.8	6.637	332.6	.450	150.7							
	.216	226.8	6.019	331.9	---	---							
	.242	253.3	6.282	335.5	.406	150.3							

TABLE III.- MEASURED FLUTTER DERIVATIVES FOR THE NACA 877A008 AIRFOIL WITH SPOILERS AT THE 70-PERCENT-CHORD STATION ON THE UPPER SURFACE; $\alpha_m = 2^\circ$

|		Spoiler height 2-1/2 percent							Spoiler height 4 percent				
M	k	ω	$\left|\dfrac{dc_l}{d\alpha}\right|$	φ	$\left|\dfrac{dc_m}{d\alpha}\right|$	θ	M	k	ω	$\left|\dfrac{dc_l}{d\alpha}\right|$	φ	$\left|\dfrac{dc_m}{d\alpha}\right|$	θ
0.596	0.043	29.5	7.035	6.2	- - -	- - -	0.596	0.046	30.8	6.240	3.1	- - -	- - -
	.081	55.4	6.649	0	- - -	- - -		.083	56.0	6.187	354.6	- - -	- - -
	.120	82.2	5.682	357.0	- - -	- - -		.122	81.6	5.897	352.2	- - -	- - -
	.158	108.3	5.872	352.2	- - -	- - -		.164	110.0	5.105	343.2	- - -	- - -
	.194	132.8	5.401	342.6	- - -	- - -		.204	136.9	4.557	345.7	- - -	- - -
	.219	149.6	4.787	340.7	- - -	- - -		.226	151.7	4.422	344.5	- - -	- - -
	.262	179.0	4.750	340.9	- - -	- - -		.266	179.0	3.199	331.0	- - -	- - -
	.366	250.3	3.988	355.5	- - -	- - -							
	.386	264.0	4.086	2.9	- - -	- - -							
.693	.034	27.4	8.129	348.1	0.434	324.4	.693	.040	30.5	6.367	1.4	0.707	343.3
	.069	55.5	8.295	347.0	.463	339.8		.072	56.6	6.555	353.3	.651	333.2
	.100	79.9	6.948	337.2	- - -	- - -		.106	83.9	6.698	351.4	- - -	- - -
	.132	105.8	6.506	337.0	.496	314.1		.142	111.6	5.864	343.7	.787	313.9
	.163	130.4	6.174	335.5	- - -	- - -		.169	133.4	5.199	338.7	- - -	- - -
	.189	151.0	4.355	332.3	.708	293.2		.195	154.0	4.384	348.4	.517	324.2
	.261	208.7	3.790	350.3	.357	293.6							
	.300	239.8	4.626	353.3	- - -	- - -							
	.324	259.6	5.481	347.6	.677	285.9							
.745	.027	23.3	8.253	352.1	.396	326.1	.745	.032	27.6	7.364	352.0	.308	308.8
	.060	52.3	8.499	343.1	.347	314.3		.066	56.4	7.244	349.9	.188	268.8
	.093	80.7	7.188	337.4	- - -	- - -		.097	82.6	6.296	334.2	- - -	- - -
	.122	105.6	6.756	337.6	.505	275.7		.127	108.1	6.124	331.9	.373	259.6
	.152	132.0	6.761	331.8	- - -	- - -		.160	136.6	5.324	331.7	- - -	- - -
	.241	209.4	4.729	342.5	.406	306.3							
	.279	242.6	5.224	341.7	- - -	- - -							
	.298	258.6	4.918	353.0	.907	356.6							
.798	.028	26.1	8.672	349.8	.340	322.0	.798	.031	28.5	6.851	351.5	.607	334.0
	.059	55.5	8.353	342.0	.434	320.1		.057	52.6	6.697	345.2	.693	316.9
	.089	83.3	7.176	336.2	- - -	- - -		.089	82.1	6.358	343.1	- - -	- - -
	.113	106.1	6.684	331.8	.661	317.1		.116	107.2	6.126	333.7	.682	298.3
	.142	133.1	5.574	323.4	- - -	- - -		.151	138.7	4.273	326.4	- - -	- - -
	.195	182.1	3.963	339.6	- - -	- - -		.200	183.7	4.068	345.1	- - -	- - -
	.227	212.2	3.926	338.0	.360	349.6							
	.258	241.6	5.099	345.1	- - -	- - -							
	.283	265.1	4.983	340.1	.638	280.9							
.860	.021	21.1	7.797	7.0	.624	358.4	.860	.055	55.2	6.227	342.3	.670	321.6
	.055	55.4	7.649	355.8	.635	318.8		.081	81.2	6.138	336.1	- - -	- - -
	.083	84.2	7.140	337.4	- - -	- - -		.106	106.5	5.204	333.3	.767	264.7
	.105	106.9	6.884	327.0	.592	295.1		.152	152.5	4.821	336.4	.251	276.7
	.152	153.6	4.152	331.9	.356	216.9		.186	186.4	5.327	339.4	- - -	- - -
	.180	182.1	4.022	347.3	- - -	- - -							
	.203	206.0	5.646	338.6	.741	275.9							
	.237	239.8	5.277	333.4	- - -	- - -							
	.261	265.1	4.698	325.0	.307	192.4							
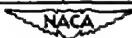
NACA

TABLE IV.- MEASURED FLUTTER DERIVATIVES FOR THE NACA 65A012 AIRFOIL WITH SPOILERS AT THE 70-PERCENT-CHORD STATION ON THE UPPER SURFACE; $\alpha_m = 2°$

| | Spoiler height 2-1/2 percent | | | | | | | Spoiler height 4 percent | | | | | |
M	k	ω	$\left|\frac{dc_l}{d\alpha}\right|$	φ	$\left|\frac{dc_m}{d\alpha}\right|$	θ	M	k	ω	$\left|\frac{dc_l}{d\alpha}\right|$	φ	$\left|\frac{dc_m}{d\alpha}\right|$	θ
0.590	0.043	29.0	6.824	1.3	---	---	0.590	0.042	28.2	6.528	3.0	---	---
	.073	48.9	6.806	358.0	---	---		.078	52.5	6.931	357.9	---	---
	.113	75.5	6.322	352.1	---	---		.117	78.2	6.184	351.0	---	---
	.153	102.5	5.765	352.1	---	---		.154	103.3	5.560	359.9	---	---
	.189	126.7	5.603	354.2	---	---		.196	131.4	5.549	356.1	---	---
	.231	154.4	5.265	347.5	---	---		.234	157.1	5.676	347.6	---	---
	.340	227.6	4.552	8.4	---	---		.343	230.2	5.199	8.7	---	---
	.380	254.4	5.181	9.3	---	---		.382	256.4	5.565	12.3	---	---
.682	.036	28.3	7.374	350.6	0.323	326.6	.682	.038	29.4	7.858	357.6	0.166	352.7
	.068	52.9	7.043	354.5	.391	328.7		.062	48.3	7.427	351.7	.262	310.2
	.100	78.4	6.519	350.1	---	---		.099	77.2	6.665	348.5	---	---
	.132	102.9	6.500	337.3	.502	291.4		.133	104.0	6.179	345.1	.445	287.0
	.166	129.6	5.992	351.0	---	---		.165	129.2	6.040	350.0	---	---
	.197	153.6	5.358	343.3	.561	279.5		.203	159.0	5.335	337.4	.469	272.9
	.294	229.3	5.172	1.7	---	---		.297	231.8	5.575	357.7	---	---
	.330	257.5	5.650	359.1	.694	276.4		.329	257.5	5.832	359.3	.858	283.5
.731	.034	28.3	8.223	2.9	.329	326.0	.731	.034	28.3	8.640	357.4	.165	343.1
	.060	50.2	7.567	354.5	.391	311.7		.061	51.0	7.638	348.9	.146	11.9
	.092	77.2	6.189	345.5	---	---		.094	78.9	6.967	341.0	---	---
	.124	104.4	6.380	345.9	.431	289.8		.126	105.9	6.470	337.9	.220	284.2
	.158	133.4	5.688	344.8	---	---		.155	130.9	6.405	341.6	---	---
	.248	208.7	5.111	333.9	.608	275.9		.243	204.6	5.278	344.7	.610	276.1
	.281	237.1	5.482	356.6	---	---		.274	231.0	5.655	350.5	---	---
	.303	255.4	5.791	355.7	.873	286.8		.301	253.3	5.758	355.5	.831	279.8
.765	.032	28.3	8.310	359.6	---	---	.765	.031	27.7	9.773	353.3	.495	181.8
	.058	51.1	7.731	350.0	---	---		.057	50.0	8.709	344.5	.216	198.1
	.088	77.9	7.682	344.2	---	---		.089	78.4	7.736	338.8	---	---
	.117	103.7	6.812	339.0	---	---		.117	103.8	7.071	335.3	.244	192.1
	.146	129.3	5.749	328.7	---	---		.145	128.7	6.479	332.2	---	---
	.231	204.6	5.700	350.1	---	---		.230	204.0	5.961	341.4	.226	238.8
	.258	228.5	5.888	353.4	---	---		.263	232.7	6.542	348.6	---	---
	.285	252.3	6.164	0.3	---	---		.284	251.3	6.950	354.8	.931	262.8
.790	.032	29.0	9.328	347.1	.292	246.0	.790	.027	25.1	9.530	0	.982	177.5
	.056	51.0	8.701	346.6	.359	229.3		.054	49.9	8.414	345.7	.868	164.1
	.087	79.4	7.445	334.3	---	---		.083	76.6	7.356	336.2	---	---
	.114	104.2	6.874	330.8	.362	210.1		.112	102.8	6.882	330.3	.514	140.3
	.143	130.6	5.492	328.4	---	---		.141	129.5	5.455	332.3	---	---
	.195	178.5	5.419	353.6	---	---		.197	181.0	5.485	353.9	---	---
	.219	200.7	4.795	340.1	.399	260.5		.221	202.6	5.102	344.1	.144	11.6
	.254	232.7	5.700	346.0	---	---		.253	232.7	7.066	348.0	---	---
	.279	255.4	6.697	346.4	.779	233.2		.275	252.3	8.708	348.7	.421	189.4
.802	.030	28.0	9.836	349.3	.730	196.0	.802	.027	24.9	9.965	345.7	1.375	141.3
	.054	50.3	9.221	337.8	.871	171.8		.056	52.5	9.077	337.1	1.103	128.7
	.083	77.7	8.483	325.9	---	---		.086	80.3	8.279	330.7	---	---
	.109	101.7	7.641	322.6	.623	157.3		.113	105.6	7.894	333.4	.591	112.1
	.140	130.6	5.625	315.6	---	---		.140	130.9	6.545	332.4	---	---
	.194	181.1	5.676	338.8	---	---		.195	182.1	6.009	345.1	---	---
	.218	203.3	4.761	349.6	.956	332.2		.214	199.4	6.152	338.9	.228	305.0
	.247	230.2	6.917	340.3	---	---							
	.267	249.3	7.967	352.5	1.318	290.5							
.837	.026	25.5	12.336	335.3	2.448	156.0							
	.053	51.4	9.849	318.2	2.234	118.8							
	.078	76.3	7.197	310.6	---	---							
	.105	102.7	7.320	311.0	2.026	95.4							
	.189	184.8	4.022	336.6	---	---							
	.206	201.4	4.995	339.3	.163	286.4							
	.237	231.8	6.141	336.1	---	---							
	.269	262.7	5.767	335.9	.456	199.5							
.857	.027	27.5	10.125	343.5	1.645	160.9							
	.051	51.1	7.283	333.3	.407	153.2							
	.077	77.8	6.147	324.5	---	---							
	.101	101.7	4.833	328.8	.390	80.6							
	.154	155.1	4.187	344.8	.463	6.7							
	.179	179.5	3.906	357.4	---	---							
	.206	207.3	5.410	355.4	.633	299.1							
	.232	233.5	5.521	350.7	---	---							
	.259	260.7	5.400	347.5	1.082	307.5							
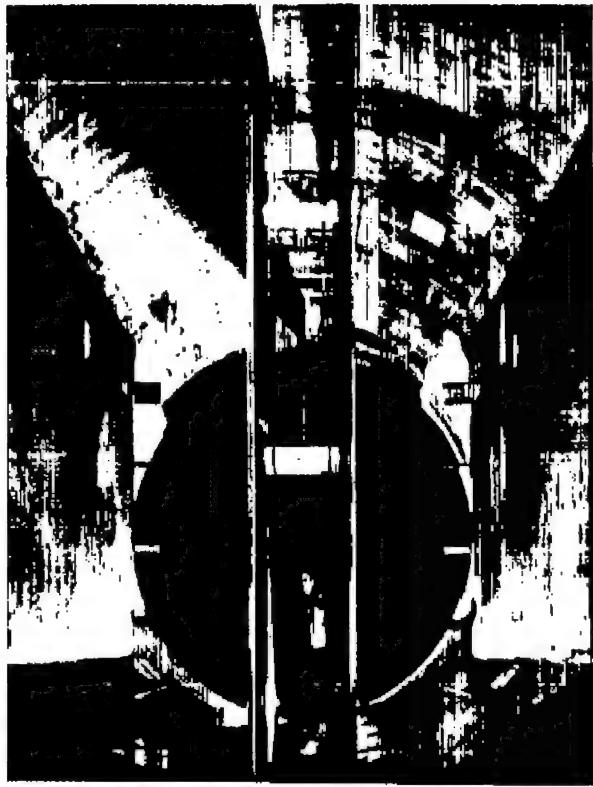
(a) Downstream view.
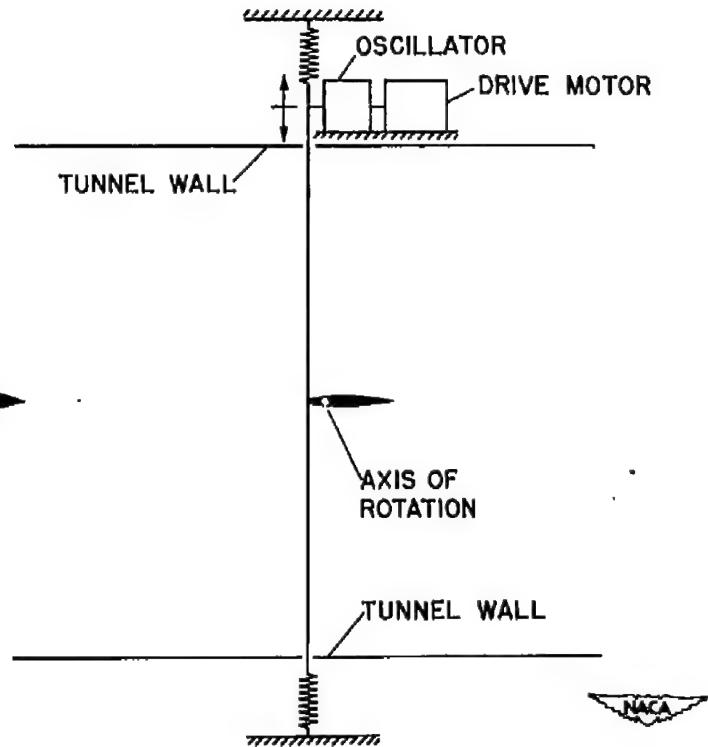
(b) Drive system.

Figure 1.- View of test section with model in place, and diagrammatic sketch of drive system.

NACA 65A012

NACA 2-008   NACA 65A008   NACA 877A008
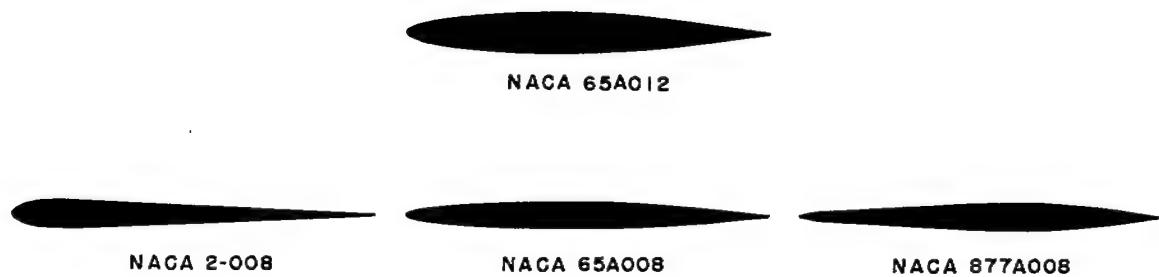
MODEL PRESSURE-CELL LOCATIONS
[In percent of model chord]

Cell no. upper and lower surface	65A012 and 65A008	2-008 and 877A008
1	1.25	1.25
2	3.75	3.75
3	7.5	7.5
4	15	15
5	22.5	22.5
6	27.5	27.5
7	35	35
8	45	45
9	52.5	52.5
10	57.5	57.5
11	62.5	62.5
12	67.5	67.5
13	75	75
14	85	85
15	95	90

Figure 2.- Section profiles and pressure-cell locations of models.
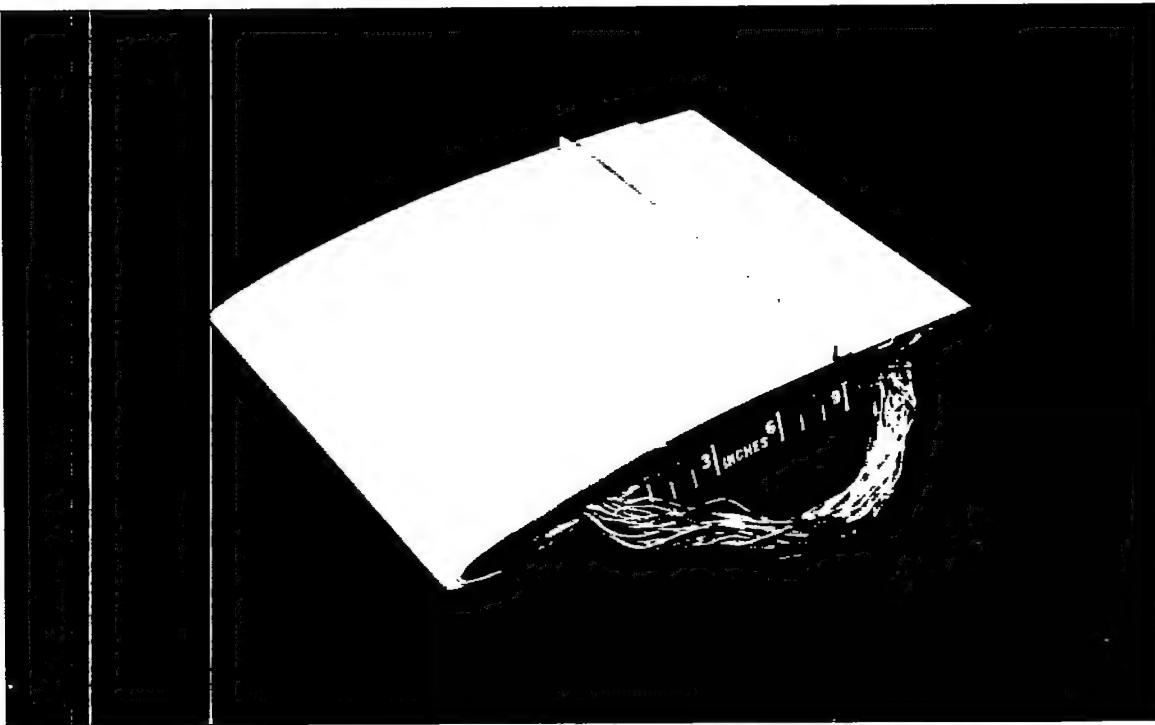
A-19114.1

Figure 3.- NACA 65A012 airfoil with spoiler mounted at the 70-percent-
chord station.
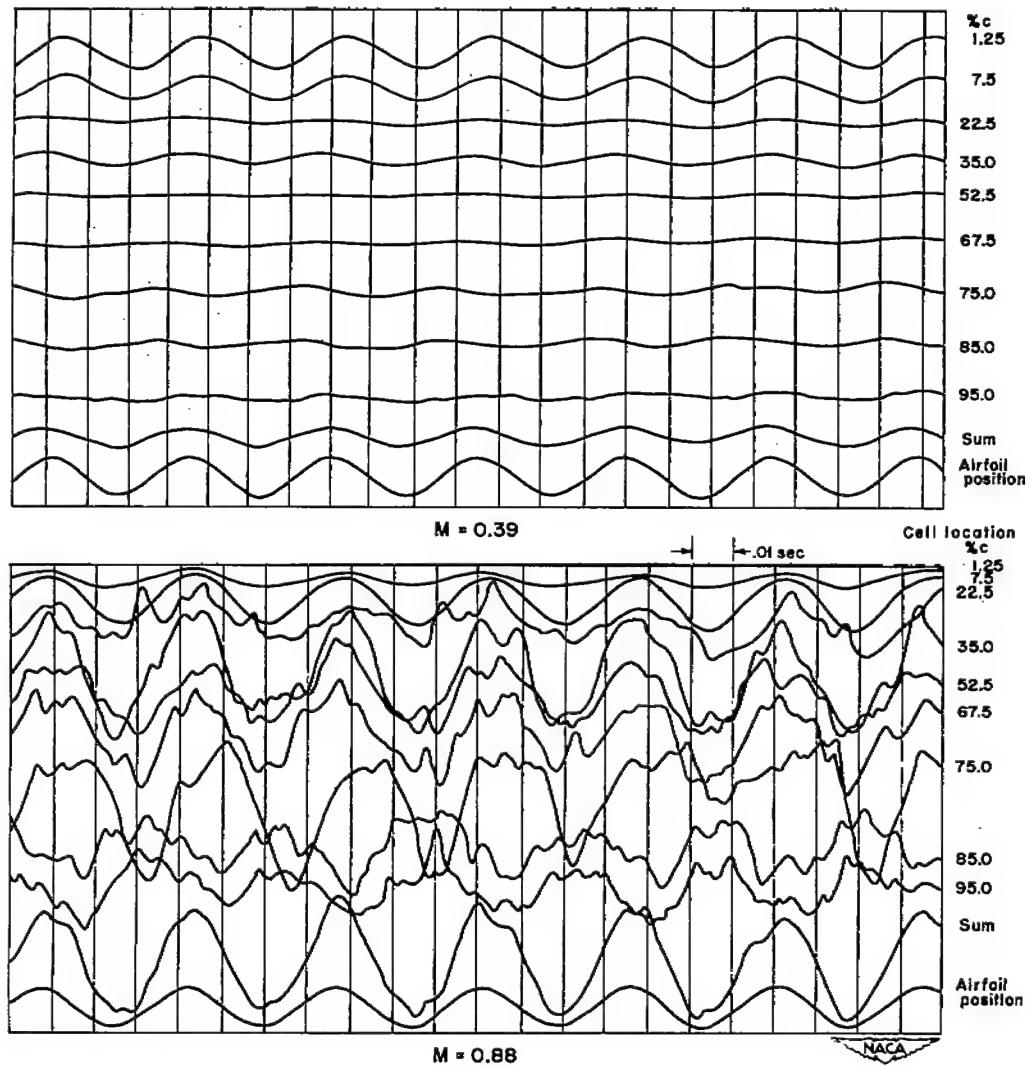
Figure 4.- Sample Oscillograms for the NACA 2-008 airfoil.
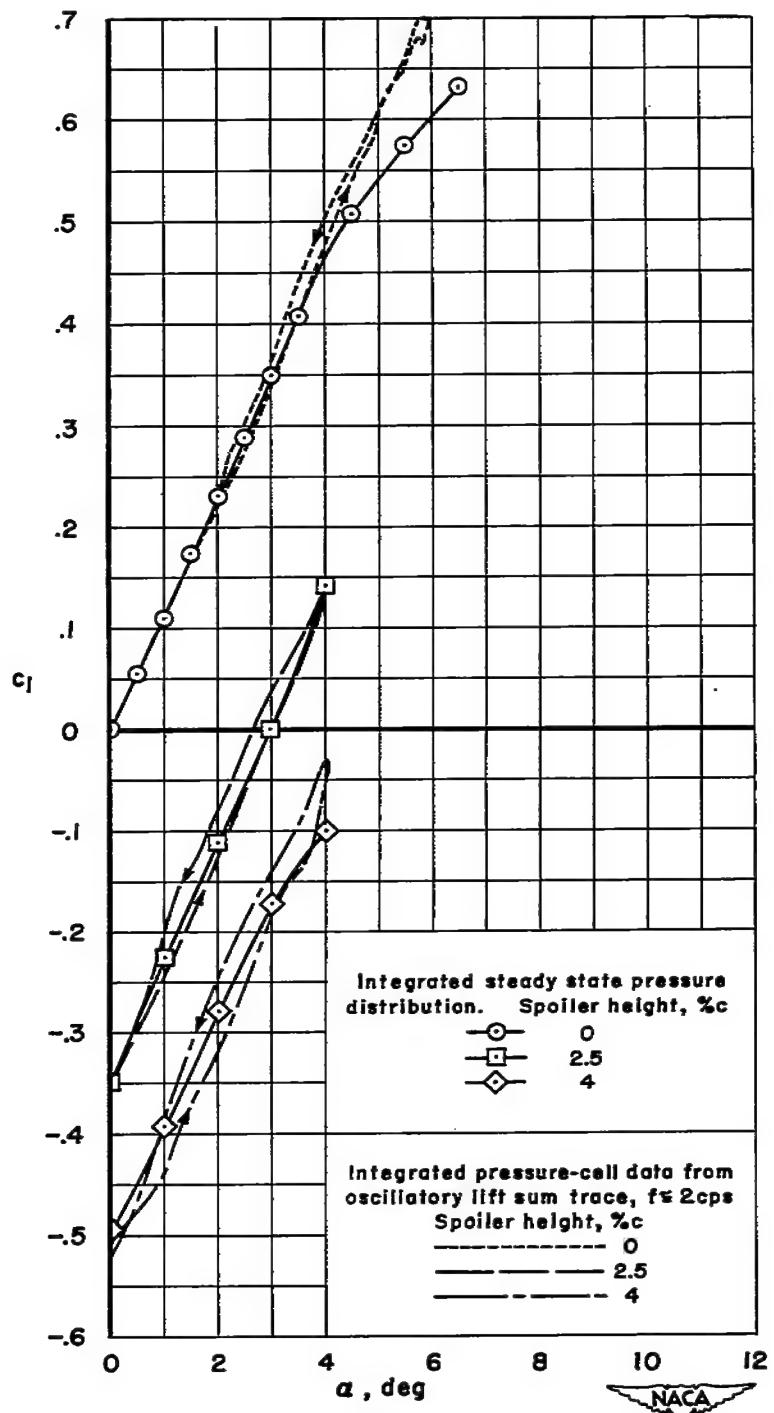
Figure 5.- Effect of spoiler deflection on the aerodynamic
lift characteristics of the NACA 65A008 airfoil;
M = 0.59.
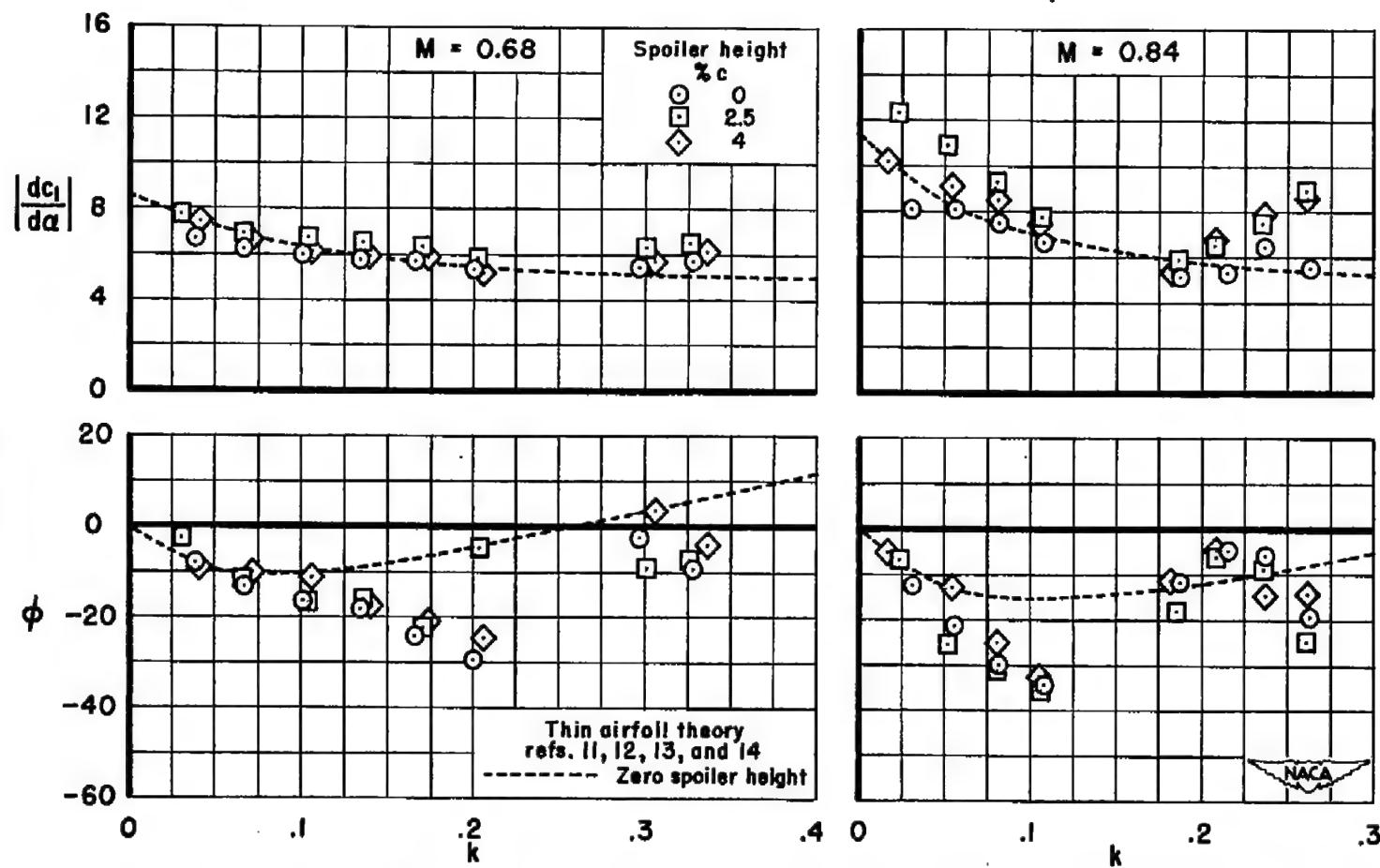
Figure 6.- Lift flutter derivative and phase angle as a function of reduced frequency for two Mach numbers for the NACA 65A008 airfoil; $\alpha_m = 2°$.
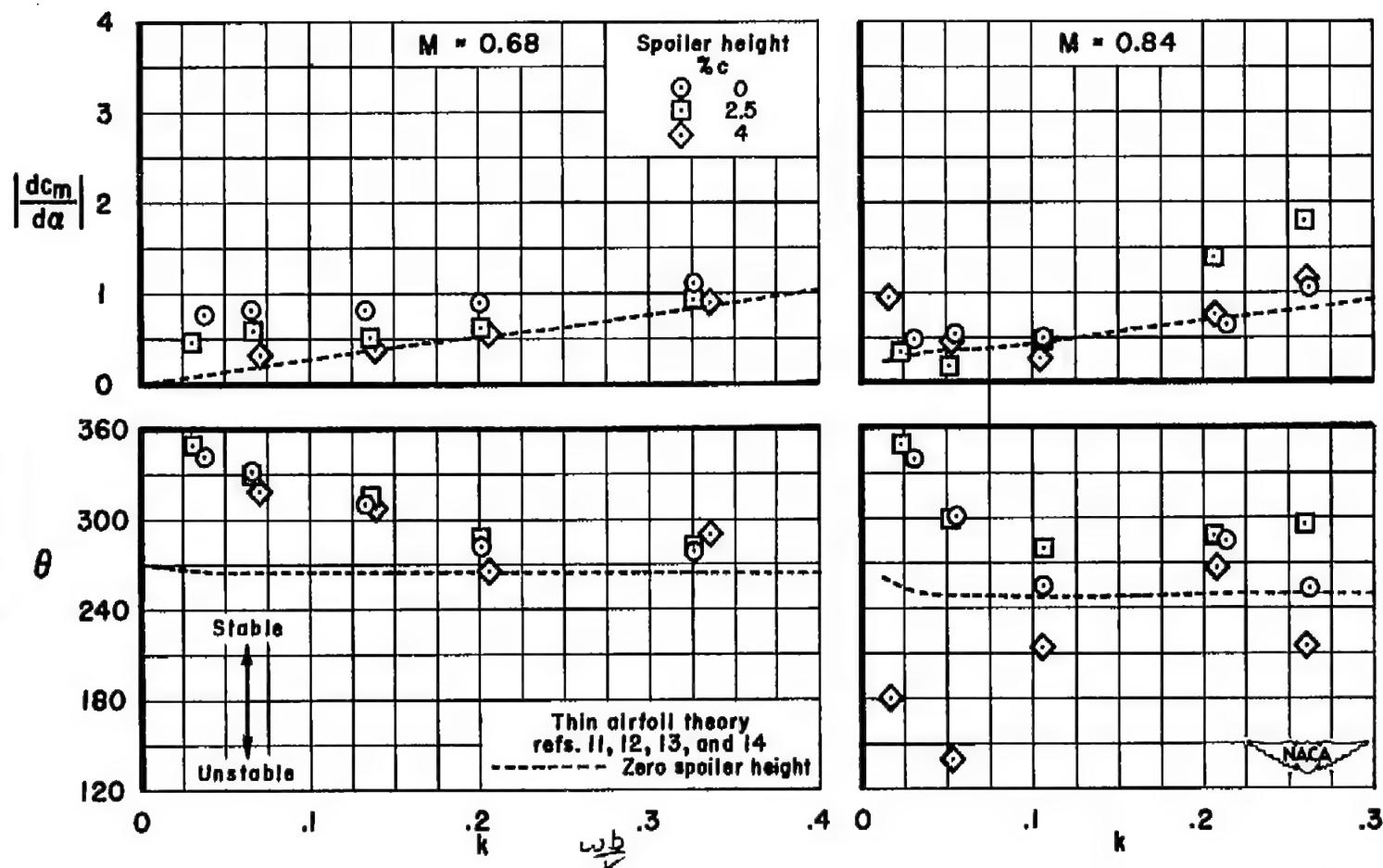
Figure 7.- Moment flutter derivative and phase angle as a function of reduced frequency for two Mach numbers for the NACA 65A008 airfoil; $\alpha_m = 2°$.
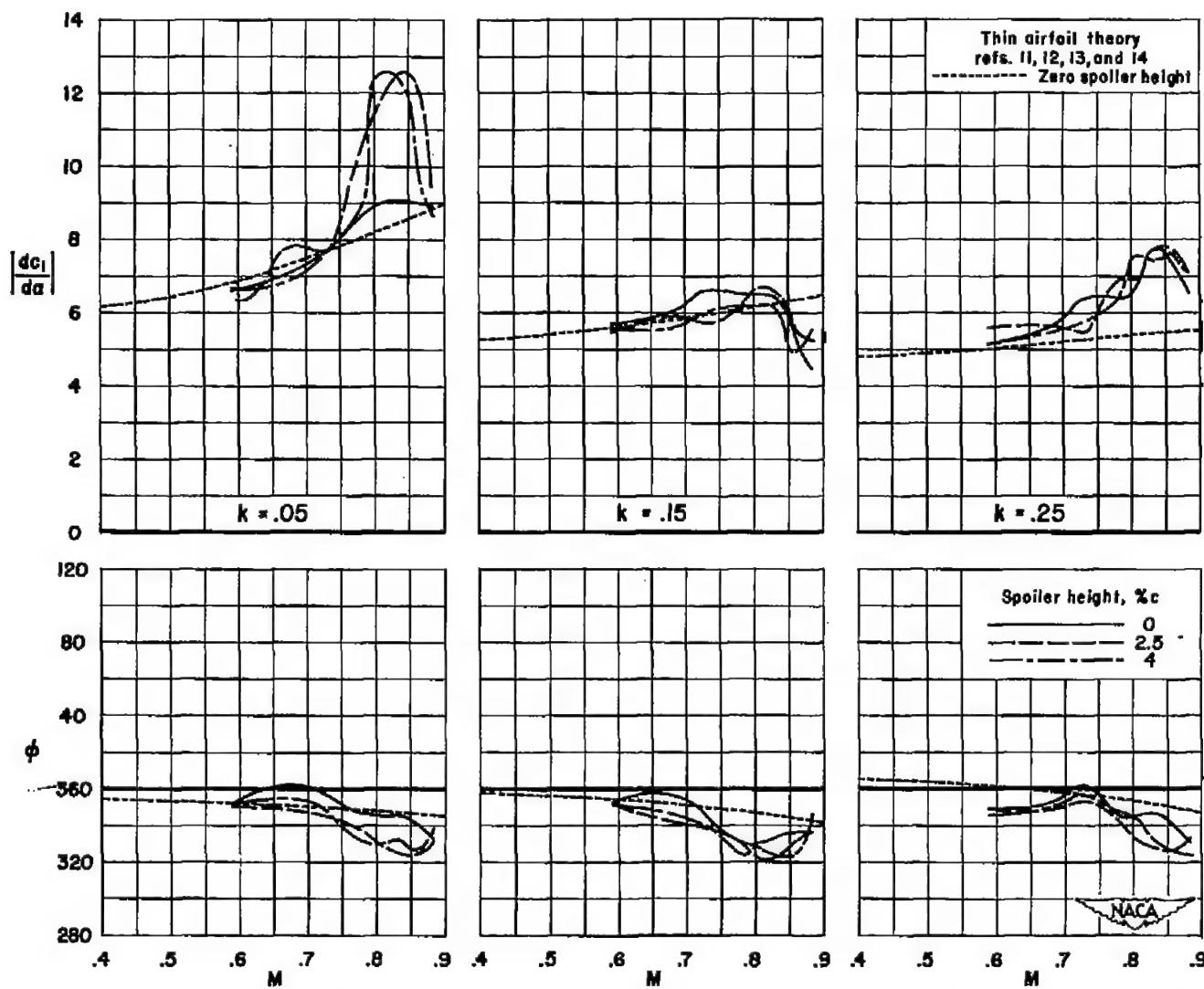
Figure 8.- Effect of fixed spoiler deflections on the lift flutter derivative and phase angle for the NACA 2-008 airfoil; $a_m = 2°$.
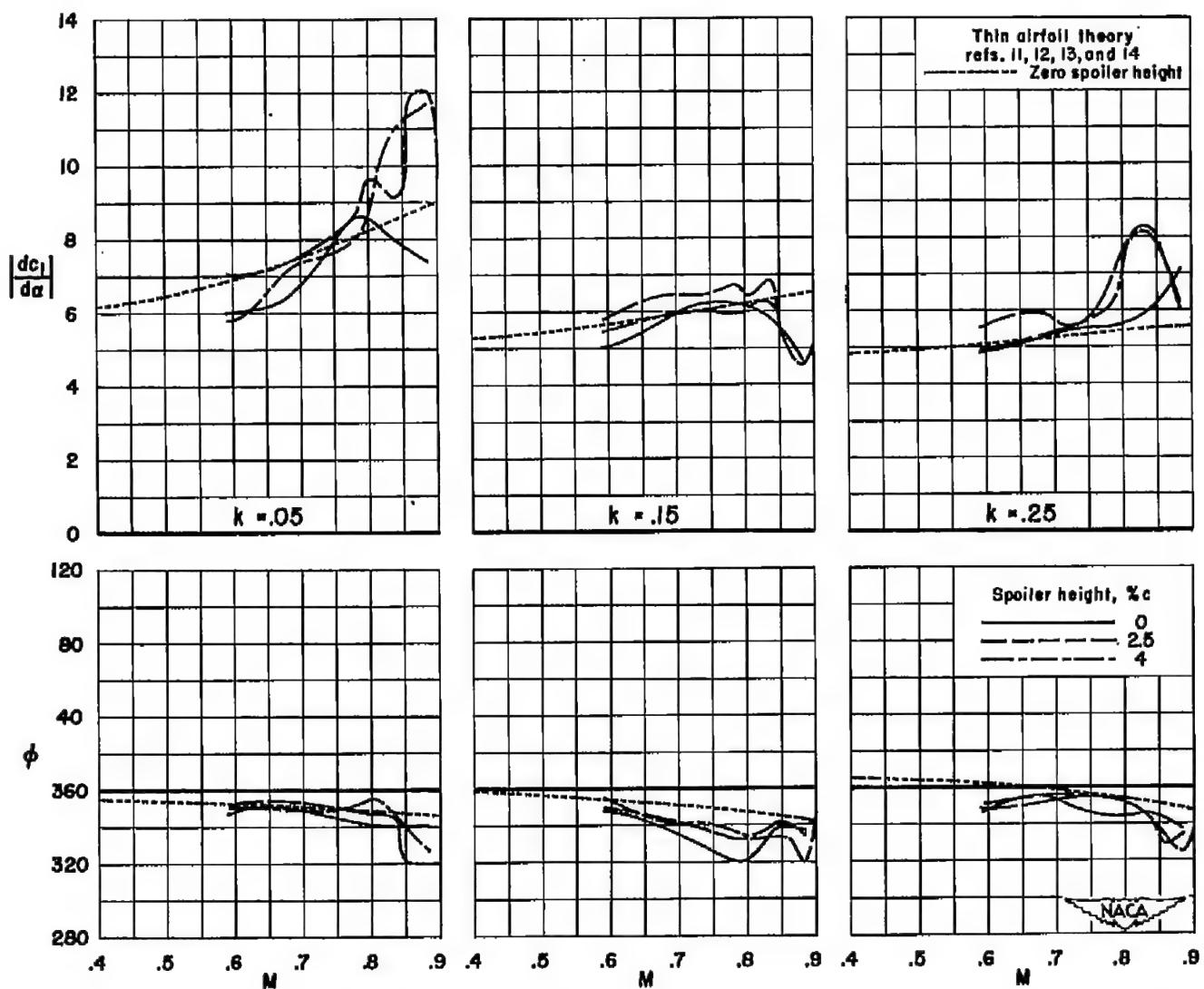
Figure 9.- Effect of fixed spoiler deflections on the lift flutter derivative and phase angle for the NACA 65A008 airfoil; $a_m = 2°$.
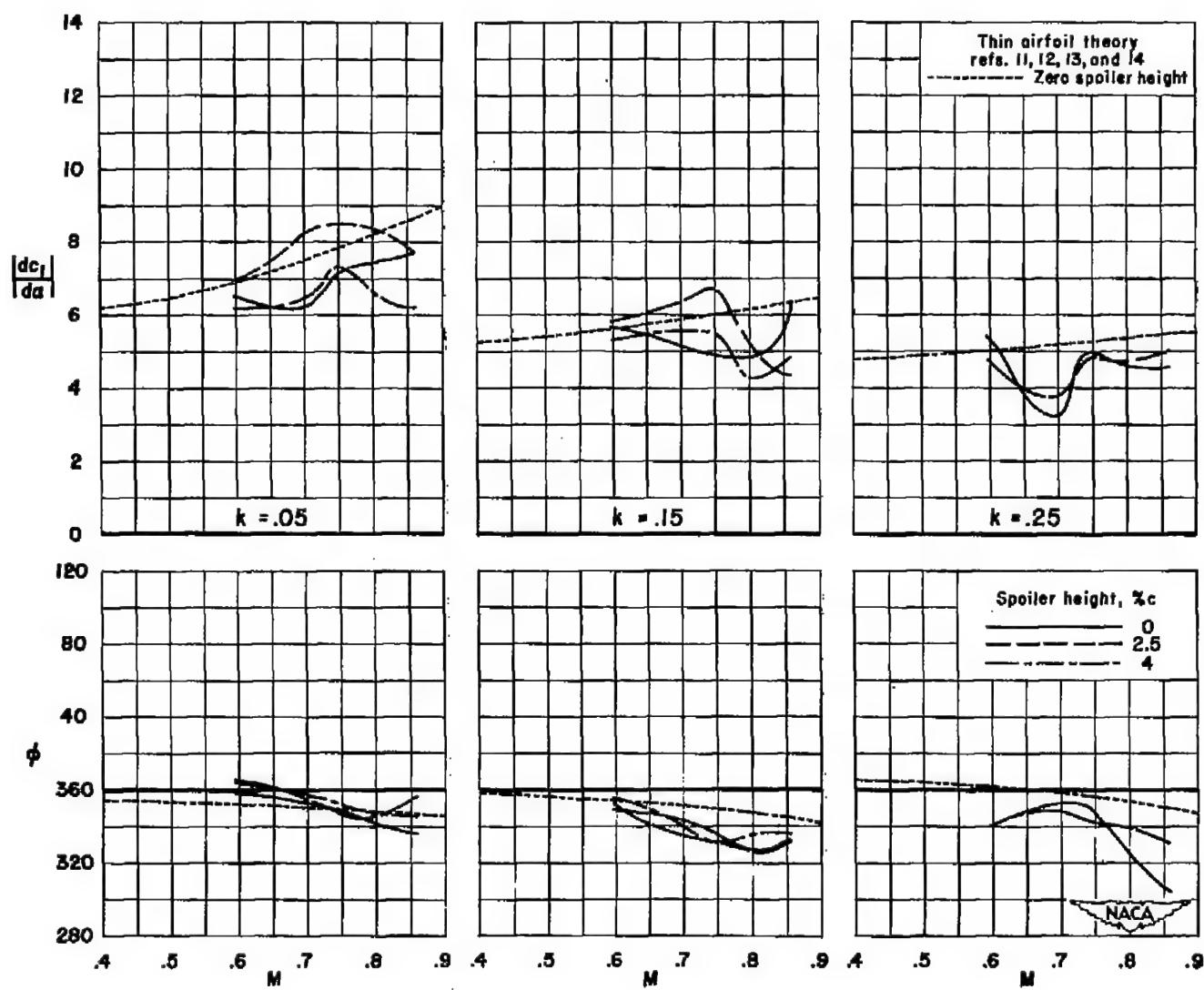
Figure 10.- Effect of fixed spoiler deflections on the lift flutter derivative and phase angle for the NACA 877A008 airfoil; $a_m = 2°$.
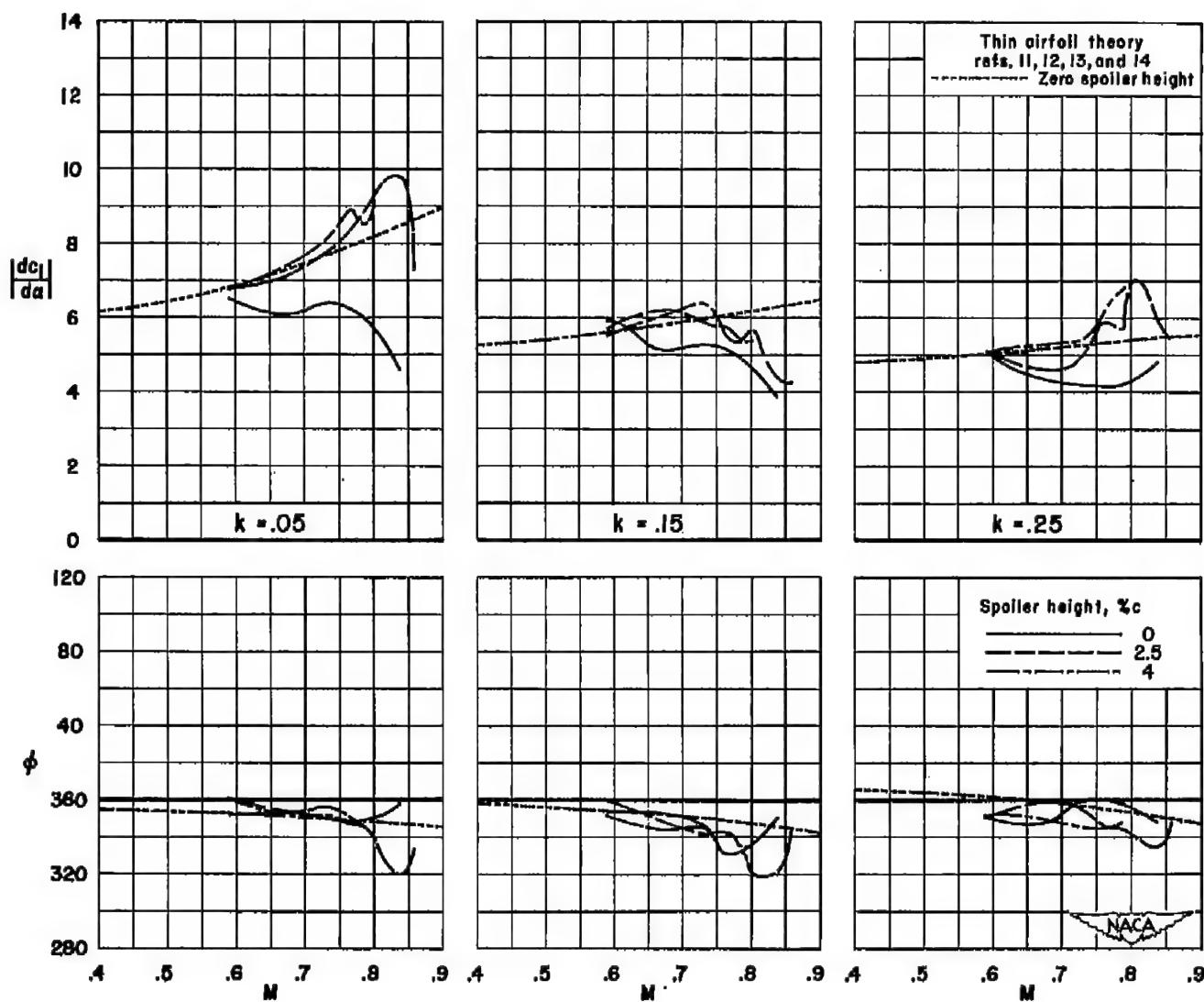
Figure 11.- Effect of fixed spoiler deflections on the lift flutter derivative and phase angle for the NACA 65A012 airfoil; a_m = 2°.
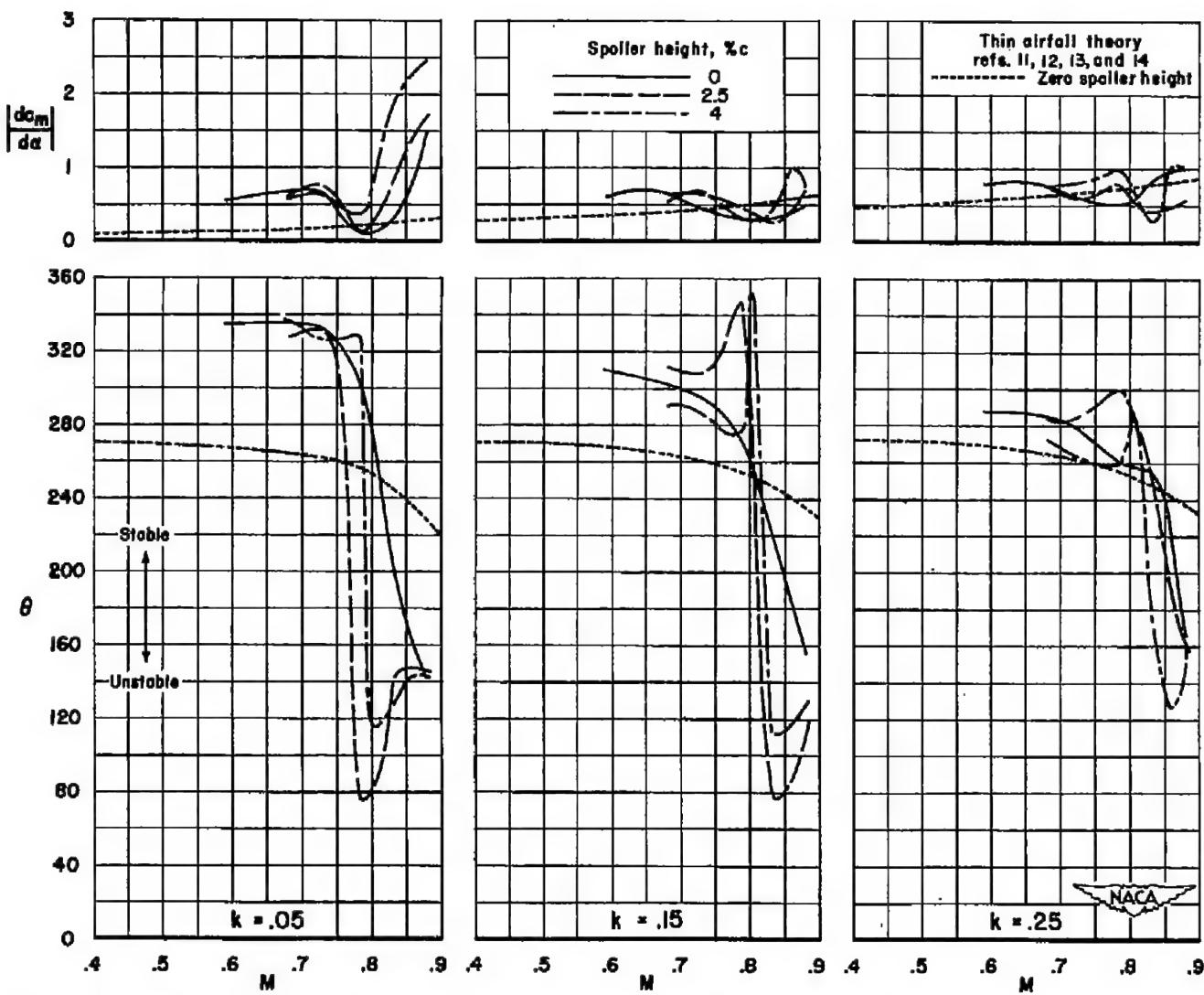
Figure 12.- Effect of fixed spoiler deflections on the moment flutter derivative and phase angle for the NACA 2-008 airfoil; $a_m = 2°$.
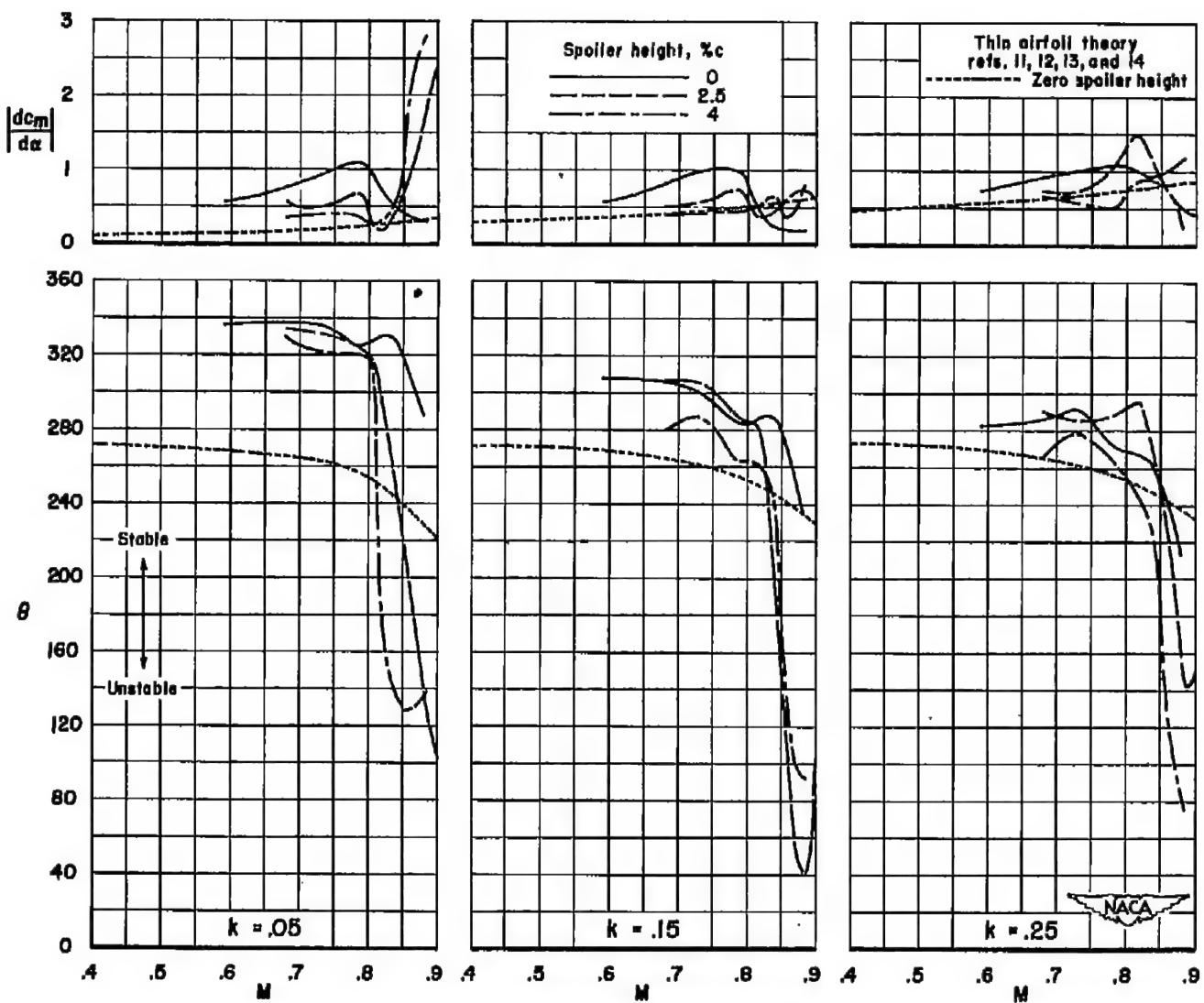
Figure 13.- Effect of fixed spoiler deflections on the moment flutter derivative and phase angle for the NACA 65A008 airfoil; $\alpha_m = 2°$.
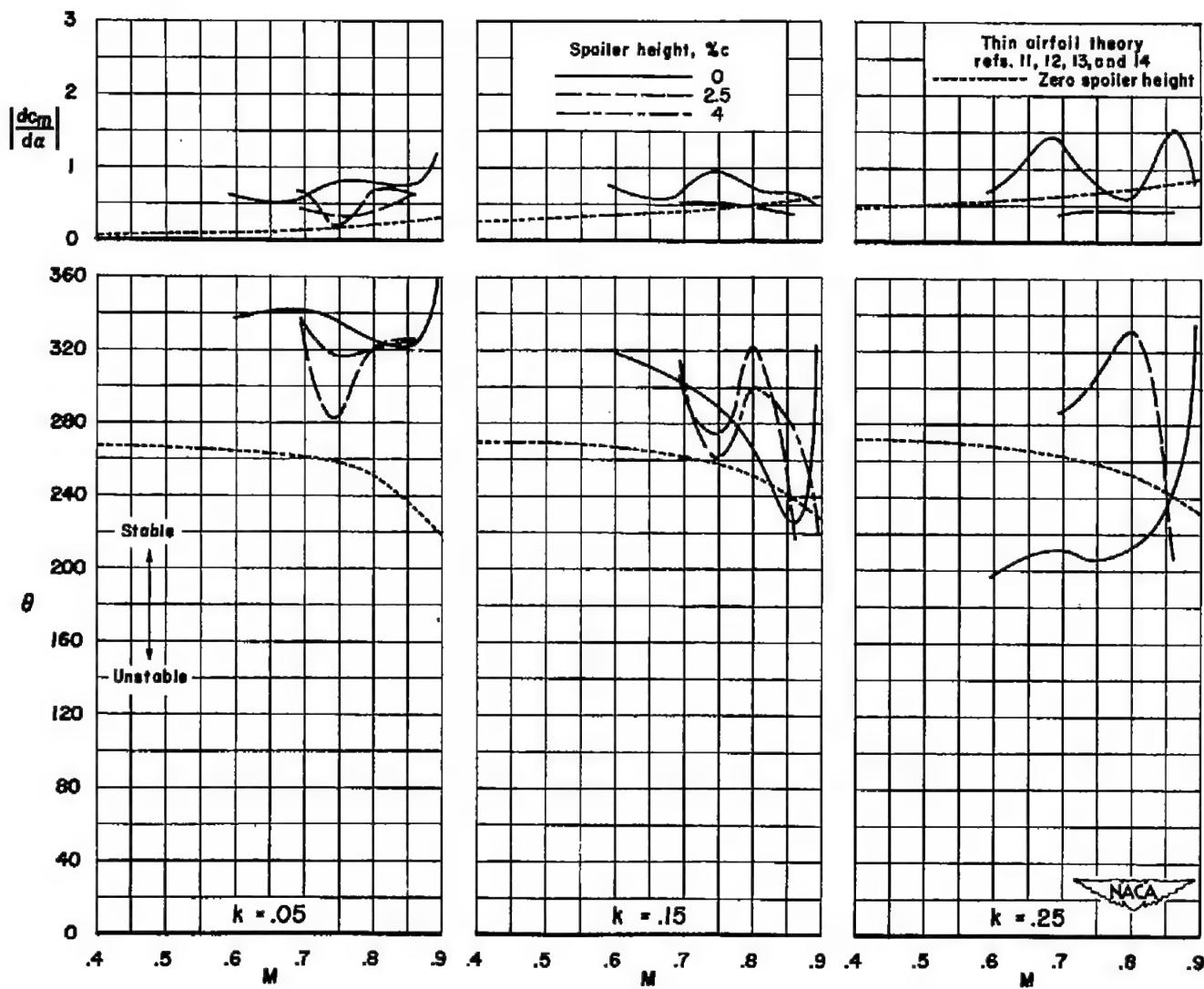
Figure 14.- Effect of fixed spoiler deflections on the moment flutter derivative and phase angle for the NACA 877A008 airfoil; $\alpha_m = 2°$.
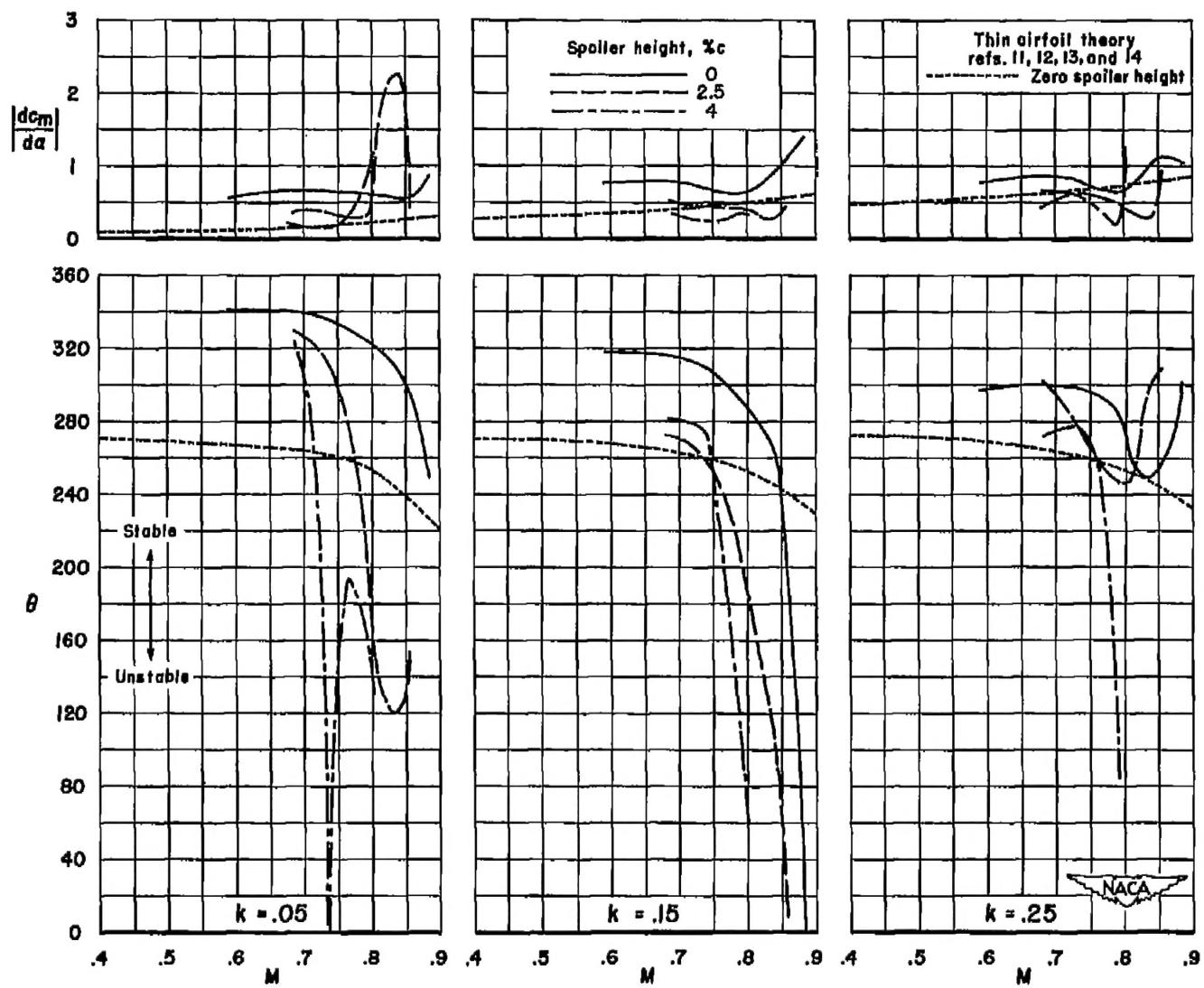
Figure 15.- Effect of fixed spoiler deflections on the moment flutter derivative and phase angle for the NACA 65A012 airfoil; $a_m = 2°$.

$$\frac{V}{\omega b}$$

NACA 2-008

Spoiler height, %c
————————— 0
——— — — 2.5
——— · — — 4

NACA 65A008

Extrap.

**NACA 877A008**

Extrapolated

NACA

.4 .5 .6 .7 .8 .9 1.0

M
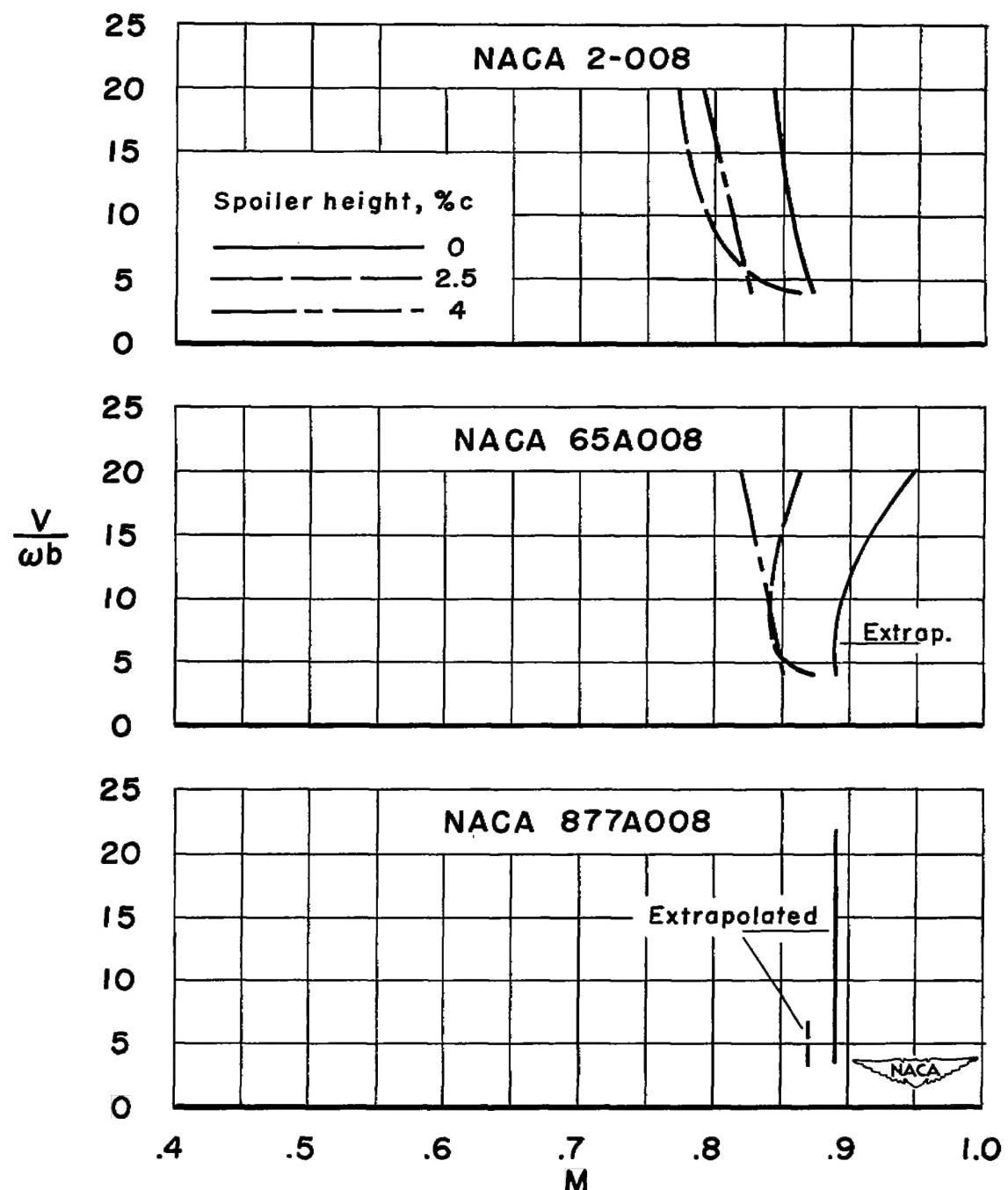
Figure 16.- Aerodynamic torsional instability boundaries as affected by airfoil thickness distribution; $\alpha_m = 2°$.
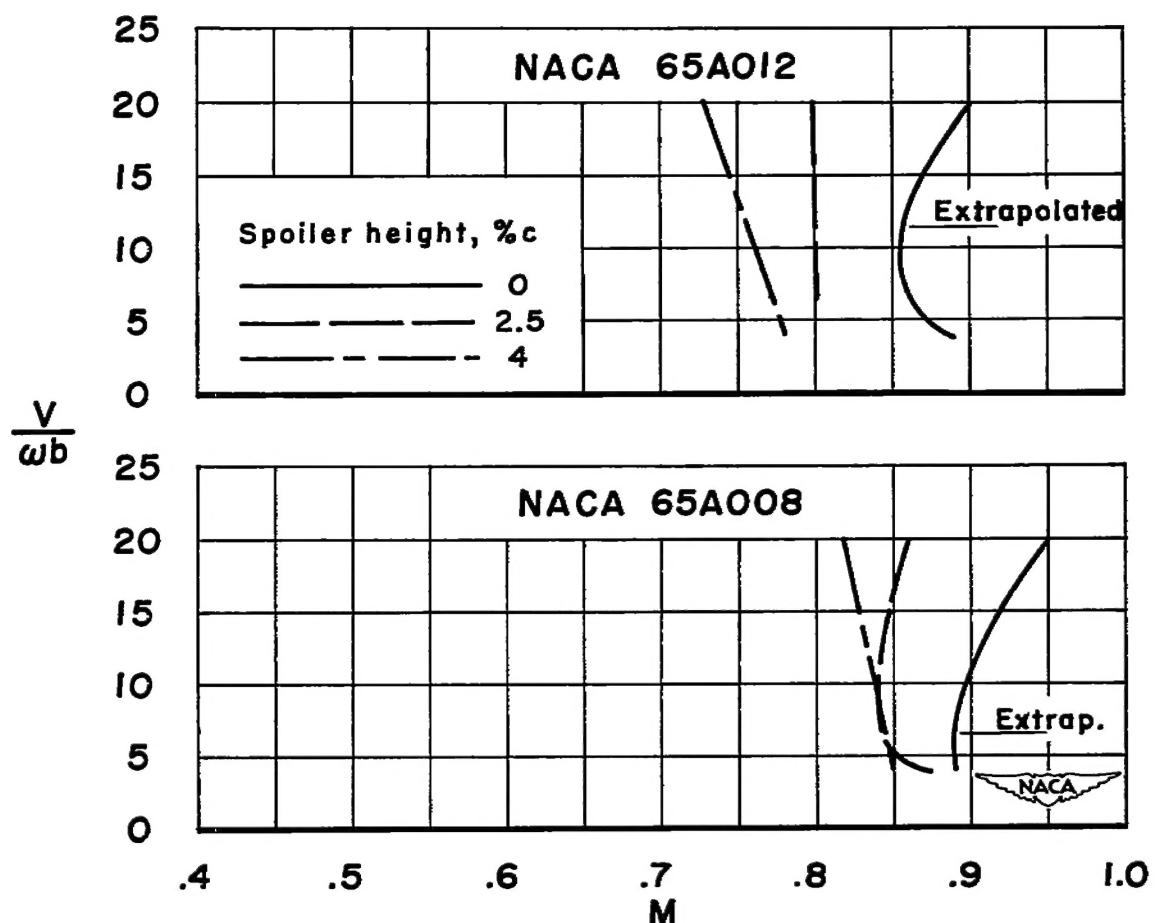
Figure 17.- Aerodynamic torsional instability boundaries as affected by airfoil thickness; $\alpha_m = 2°$.